AD-A152 712   OPERATING CHARACTERISTICS ABSORPTIVITY/REFLECTIVITY MEASUREMENTS AND PULS..(U) NAVAL POSTGRADUATE SCHOOL MONTEREY CA   E L GARCIA DEC 84   1/1

UNCLASSIFIED   F/G 20/5   NL

END

FILMED

DTIC

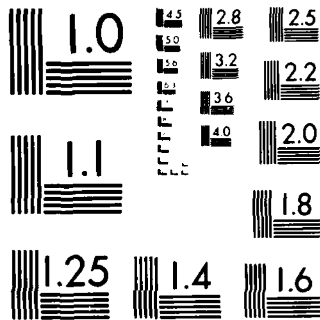

MICROCOPY RESOLUTION TEST CHART
NATIONAL BUREAU OF STANDARDS 1963 A

AD-A152 712

NAVAL POSTGRADUATE SCHOOL

Monterev California

THESIS

OPERATING CHARACTERISTICS, ABSORPTIVITY/REFLECTIVITY MEASUREMENTS, AND PULSE SYSTEM DESIGN OF THE NPS HYDROGEN FLUORIDE/DEUTERIUM FLORIDE LASER

by

Edward Lee Garcia

December 1984

Thesis Advisor: A. W. Cooper

DTIC FILE COPY

APR 24 1985
D
A

Approved for public release; distribution is unlimited.

UNCLASSIFIED

SECURITY CLASSIFICATION OF THIS PAGE (When Data Entered)

REPORT DOCUMENTATION PAGE

READ INSTRUCTIONS BEFORE COMPLETING FORM

1. REPORT NUMBER	2. GOVT ACCESSION NO. A152 112
3. RECIPIENT'S CATALOG NUMBER	
4. TITLE (and Subtitle) Operating Characteristics, Absorptivity/Reflectivity Measurements; and Pulse System Design of the NPS Hydrogen Fluoride/Deuterium Fluoride Laser	5. TYPE OF REPORT & PERIOD COVERED Master's Thesis December 1984
	6. PERFORMING ORG. REPORT NUMBER
7. AUTHOR(s) Edward Lee Garcia	8. CONTRACT OR GRANT NUMBER(s)
9. PERFORMING ORGANIZATION NAME AND ADDRESS Naval Postgraduate School Monterey, CA 93943-5100	10. PROGRAM ELEMENT, PROJECT, TASK AREA & WORK UNIT NUMBERS
11. CONTROLLING OFFICE NAME AND ADDRESS Naval Postgraduate School Monterey, CA 93943-5100	12. REPORT DATE December 1984
	13. NUMBER OF PAGES 59
14. MONITORING AGENCY NAME & ADDRESS (if different from Controlling Office)	15. SECURITY CLASS. (of this report)
	15a. DECLASSIFICATION DOWNGRADING SCHEDULE

16. DISTRIBUTION STATEMENT (of this Report)

Approved for public release; distribution is unlimited.

17. DISTRIBUTION STATEMENT (of the abstract entered in Block 20, if different from Report)

18. SUPPLEMENTARY NOTES

19. KEY WORDS (Continue on reverse side if necessary and identify by block number)

Hydrogen Fluoride/Deuterium Fluoride Laser
Absorptivity/Reflectivity

20. ABSTRACT (Continue on reverse side if necessary and identify by block number)

The Hydrogen Fluoride/Deuterium Fluoride Laser is a fast flow electrical discharge operated chemical laser. Refitting of the subsystems of the laser was completed and lasing was observed utilizing a 100 percent reflectance mirror and a 95 percent reflectance output coupling mirror. The maximum multiline output power obtained was 2.6 Watts at 19.0 kV and 475 mA. The data obtained was in general agreement with previously reported data. However, an increase in power output from 1.6 to 2.6 Watts was obtained by

DD FORM 1473 1 JAN 73 EDITION OF 1 NOV 65 IS OBSOLETE

S N 0102-LF-014-6601

UNCLASSIFIED

SECURITY CLASSIFICATION OF THIS PAGE (When Data Entered)

utilization of a Hipotronics power supply that enabled usage of higher input voltages for SF_6 dissociation. Measurements were also taken over a variation of the [illegible], SF_6, H_2, and O_2 flow rates resulting in the change of the optimum flow r[illegible]s for the above listed gases. The new flows were found to be (1) SF_6=.71[illegible] grams/second (2) H_2=.0220 grams/second (3) O_2=.22 grams/second and (4) He=.05 grams/second.

Target reflectivity/absorptivity measurements were taken and a dependence on incidence angle with the laser beam was found. For the P-doped Silicon wafer used, the power absorbed decreased over the range of 25 to 60 degrees. At the 25 degree angle approximately 95 percent of the incident power was absorbed. The reflected power was found to increase with the increase in target angle with approximately 95 percent of the incident power being reflected at 60 degrees. The results of these measurements are in general agreement with previously reported measurements.

A design for reconfiguring the HF/DF laser system into a pulsed system was also formulated but was not tested. The design criterian was to utilize a capacitor bank to drop a high voltage pulse across the anodes of the laser.

Approved for public release; distribution is unlimited.

Operating Characteristics, Absorptivity/Reflectivity Measurements, and Pulse System Design of the NPS Hydrogen Fluoride/Deuterium Fluoride Laser

by

Edward Lee Garcia
Lieutenant, United States Navy
B.S., United States Naval Academy, 1977

Submitted in partial fulfillment of the requirements for the degree of

MASTER OF SCIENCE IN PHYSICS

from the

NAVAL POSTGRADUATE SCHOOL
December 1984

Author: Edward Lee Garcia

Approved by: A.W. Cooper, Thesis Advisor

E.A. Milne, Second Reader

G.E. Schacher, Chairman, Department of Physics

J.N. Dyer, Dean of Science and Engineering

ABSTRACT

The Hydrogen Fluoride/Deuterium Fluoride Laser is a fast flow electrical discharge operated chemical laser. Refitting of the subsystems of the laser was completed and lasing was observed utilizing a 100 percent reflectance mirror and a 95 percent reflectance output coupling mirror. The maximum multiline output power obtained was 2.6 Watts at 19.0 kV and 475 mA. The data obtained was in general agreement with previously reported data. However, an increase in power output from 1.6 to 2.6 Watts was obtained by utilization of a Hipotronics power supply that enabled usage of higher input voltages for SF_6 dissociation. Measurements were also taken over a variation of the He, SF, H, and 0 flow rates resulting in the change of the optimum flow rates for the above listed gases. The new flows were found to be (1) SF_6 =.7167 grams/second (2) H_2 =.0220 grams/second (3) O_2 =.22 grams/ second and (4) He = .05 grams/second.

Target reflectivity/absorptivity measurements were taken and a dependence on incidence angle with the laser beam was found. For the P-doped Silicon wafer used, the power absorbed decreased over the range of 25 to 60 degrees. At the 25 degree angle approximately 95 percent of the incident power was absorbed. The reflected power was found to increase with the increase in target angle with approximately 95 percent of the incident power being reflected at 60 degrees. The results of these measurements are in general agreement with previously reported measurements.

A design for reconfiguring the HF/DF laser system into a pulsed system was also formulated but was not tested. The design criterian was to utilize a capacitor bank to drop a high voltage pulse across the anodes of the laser.

TABLE OF CONTENTS

I. INTRODUCTION 9
A. HISTORICAL INFORMATION AND BACKGROUND 9
B. THEORY OF OPERATION 11

II. LASER DESIGN 26
A. INTRODUCTION 26
B. REGIONS OF THE HF/DF LASER 27
1. Discharge Region 27
2. Inlet Region 29
3. Lasing Zone 29
4. Heat Exchanger Region 29
5. Exhaust Region 29

III. OPERATING CHARACTERISTICS 34
A. INTRODUCTION TO HF OPERATION 34
B. HF MULTILINE OPERATION 34
C. TARGET REFLECTIVITY/ABSORPTIVITY 37
D. PULSE SYSTEM LASER DESIGN 39

IV. CONCLUSIONS 51
A. LASER OPERATING CHARACTERISTICS 51
B. POWER VARIATION WITH TARGET ANGLE 51
C. PULSE SYSTEM DESIGN 52
D. RECOMMENDATIONS FOR FURTHER STUDY 52

APPENDIX A: START UP PROCEDURES 54

APPENDIX B: SHUT DOWN PROCEDURES 55

APPENDIX C: LASER CAVITY ALIGNMENT 56

LIST OF REFERENCES 58

INITIAL DISTRIBUTION LIST 59

LIST OF TABLES

I. Thermally Driven Lasers 19
II. Electrical Discharge Driven Lasers 20
III. Reactions for $F+H_2$ Laser 22
IV. Approximate Flow Rates for Steel Ball Readings . . 41

LIST OF FIGURES

1.1 Reaction Coordinate Diagrams 23
1.2 Population Densities 24
1.3 HF Premixed and Mixing Options 25
2.1 The NPS HF/DF Laser System 31
2.2 HF/DF Laser Regions 32
2.3 Hipotronics Power Supply 33
3.1 Power Variation with SF_6 Flow 42
3.2 Power Variation with H_2 Flow 43
3.3 Power Variation with O_2 Flow 44
3.4 Power Variation with He Flow 45
3.5 Power Variation with Input Voltage 46
3.6 Laser/Target Interaction Diagram 47
3.7 Power Reflected vs Target Angle 48
3.8 Power Absorbed vs Target Angle 49
3.9 HF/DF Pulse Laser System Design 50

ACKNOWLEDGEMENTS

During the past three years I have had the opportunity to attend the Naval Postgraduate School and become involved in the Weapons Systems Science Curriculum of the Department of Physics. This department is staffed by professors who are industrious, competent, congenial, and above all, interested in the achievement of each of their individual students. It has been a pleasure and inspiration to study and learn in such an atmosphere of education.

I am very grateful for the advice, encouragement, and education provided by the professors in the Physics department and in particular----Professors A.W. Cooper, E.A. Milne, and D.F. Walters.

I would also like to acknowledge and thank the friends who have contributed to my research efforts on the HF/DF laser and thus to the production of this thesis----Bob Sanders, whose advice, assistance in data compilation, and electronic and optics knowledge enabled me to actually achieve laser output from the HF/DF laser after it had been sitting idle for a period of seven years, and also to Bob Moeller for his painstaking effort in fabricating and machining material that was required for the lasing of the HF/DF laser.

Finally, I would like to thank my wife, Debra, for putting up with all the long and lonely nights she spent while I was working on this research project and also for her love and encouragement during the past three years.

I. INTRODUCTION

A. HISTORICAL INFORMATION AND BACKGROUND

The first chemical laser emission was experimentally observed in 1965 using a Hydrogen Chloride chemical laser [Ref. 1]. Since 1965 many chemical lasers have been developed, which can be grouped into two different classes:

1. Thermally Driven Lasers
2. Electrical Discharge Driven Lasers

Tables I and II list these developements through 1974. Our specific interest lies with the Electrical Discharge Driven Laser which will be discussed later.

The primary goal of a chemical laser is to convert chemical energy efficiently into coherent radiation of high power [Ref. 2]. The following factors must be carefully scrutinized and highly controlled to achieve this conversion efficiently.

1. The production rates of vibrationally excited molecules, Hydrogen Fluoride and/or Deuterium Fluoride (HF/DF) in our case, should be fast since these molecules are rapidly deexcited by fast collisional deactivation.
2. The temperature of the active medium must be low since a large amount of heat produced in the reaction will increase the rotational energy which will decrease the population inversions on which the laser operates.
3. The photon flux must be high and uniform in the cavity.

These controls are important for high power production, as discussed in reference 2. The control of all three of these

factors was difficult in the pulsed lasers but, because of the gas dynamic techniques utilized in the continuous wave (CW) lasers, efficient extraction of high power from chemical reactions was obtained.

Gas dynamic techniques were utilized in a chemical laser as early as 1967. The reaction of hydrogen with fluorine was known to be possible at a constant pressure in a supersonic flow thus allowing for control of the reaction and for the conversion of the energy released in the reaction to coherent radiation. Two solutions in this supersonic flow work were:

1. A free jet "flame" induced by a shock did not succeed for several reasons even with the advantages associated with it. This solution will not be discussed here.
2. A supersonic "flame" allowed a very fast mixing process in the active medium.

In 1969 lasing was observed from a supersonic diffusion flame and this has led to the developement of the high-power, high-efficiency HF/DF lasers of today [Ref. 2].

The HF/DF laser at the Naval Postgraduate School (NPS) is an Electrical Discharge Chemical Laser in which the halogen atoms are formed by an electrical discharge rather than by thermal equilibrium dissociation. The dissociation technique is accomplished at low pressures and is relatively inefficient; hence this type of CW hydrogen halide laser has an inherently low power output on the order of 1 Watt, is relatively inefficient, does not appear to be scalable to higher power, but is amplitude and frequency stable, has a low cost, high spectral line output, and high output stability [Ref. 2]. Table II lists the lasers and summarizes the experiments and results obtained until 1974 in chronological order.

There is a need for a small-scale laser. Some of the applications of this type of laser are discussed in reference 3 and are listed below [Ref. 3]

1. small-signal-gain measurements,
2. atmospheric propagation measurements,
3. window-material and optical-coating developement,
4. laser light sources for laser-induced chemistry experiments.

Other applications for the use of the small-scale chemical laser are discussed by Cool [Ref. 4] and by Hinchen [Ref. 5].

In this presentation the basic theory of operation of a chemical laser's production rates, the laser design and construction, and the operating characteristics of the NPS HF/DF laser will be discussed. From reference 6 we find that the DF laser is the most desirable laser to operate at sea level in the Infrared region and hence some useful atmospheric propagation measurements of the $P_2(8)$ transition line at 3.8007 micrometers could be performed. Another application that can be investigated is the surface reflectivity/ absorptivity, temperature rise, and thermal damage caused by irradiation of a target material.

B. THEORY OF OPERATION

The chemical laser is a very complicated system with many different types of reaction occurring simultaneously. It uses a chemical reaction to produce a population inversion between the states of the product of the reaction. The vibrational states of the molecular product are the states of major concern. The reaction is exothermal with the released energy being trapped partially or wholly in the excited states. The HF/DF laser at the Naval Postgraduate School is a hybrid laser in that the active reactants are

REPRODUCED AT GOVERNMENT EXPENSE

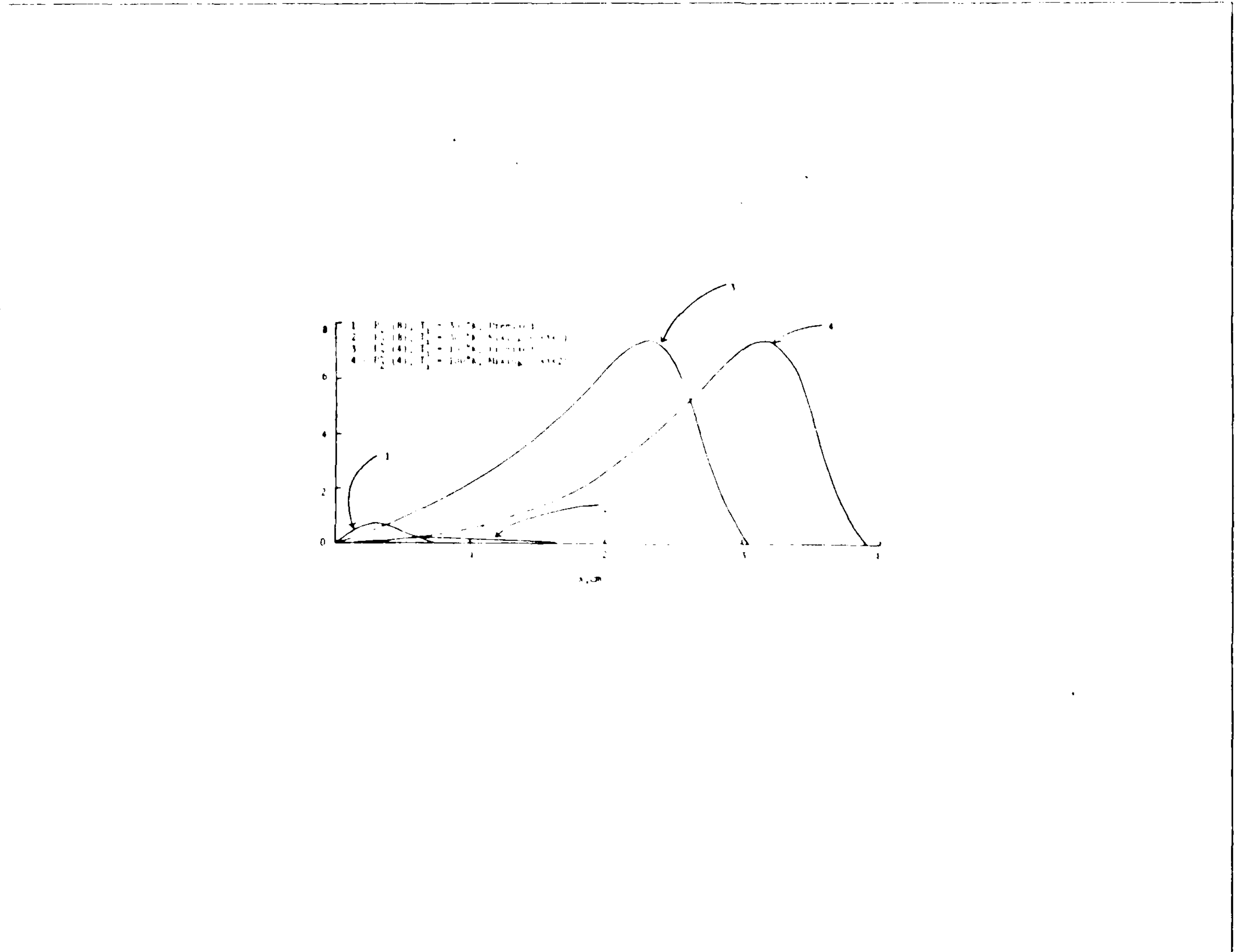

Figure 1.3 HF Premixed and Mixing Options [Ref.8]

REPRODUCED AT GOVERNMENT EXPENSE

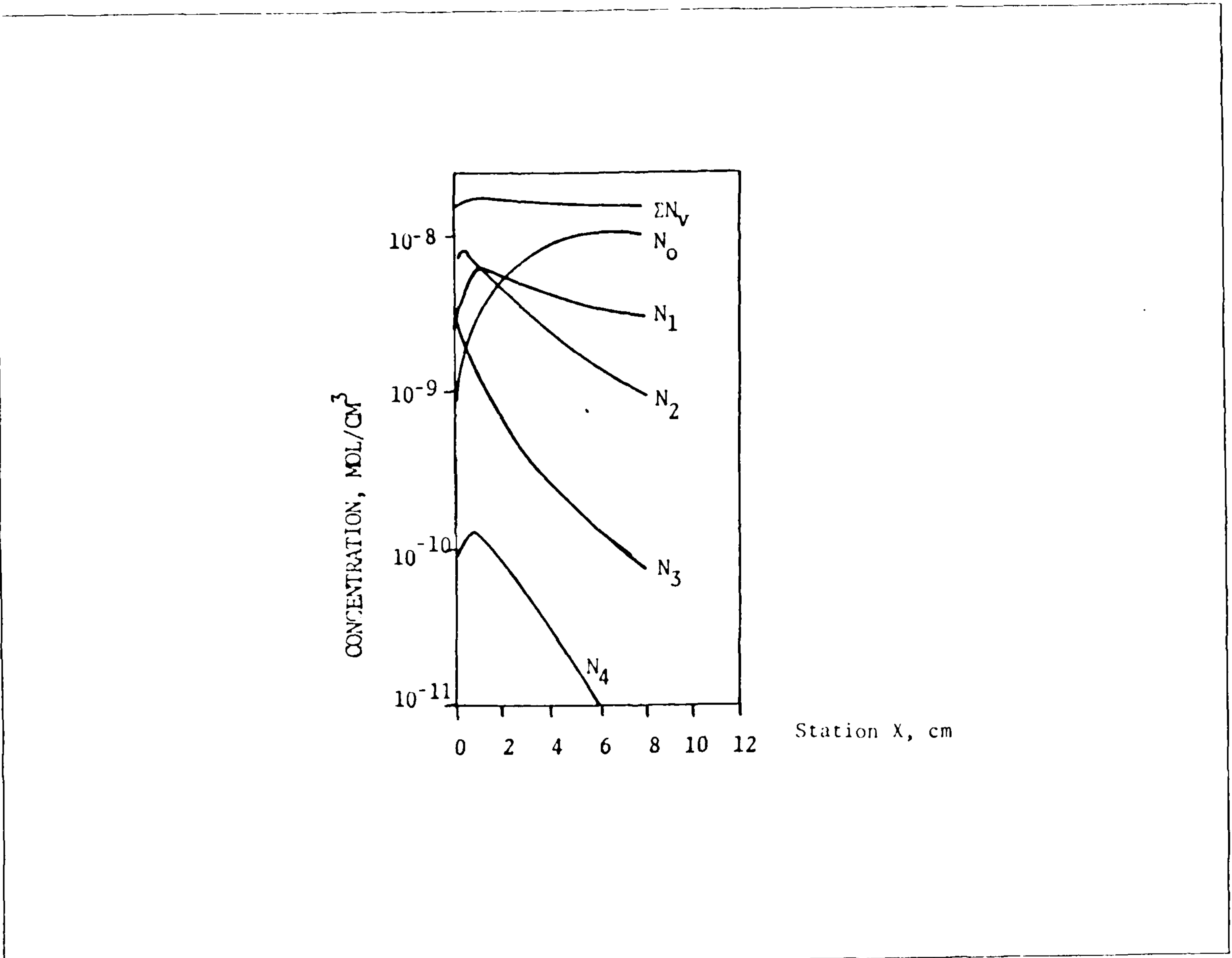

Figure 1.2 Population Densities [Ref.8]

REPRODUCED AT GOVERNMENT EXPENSE

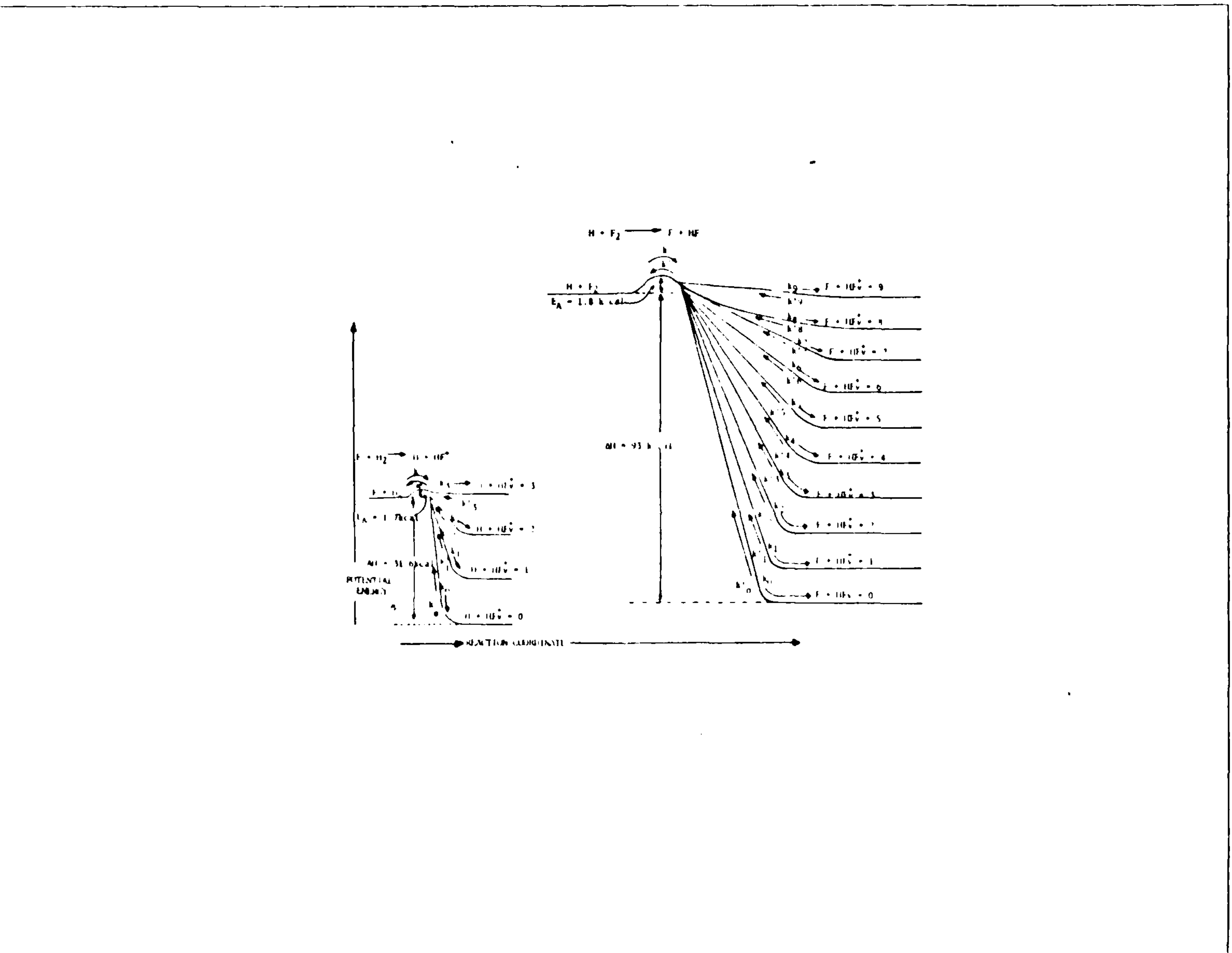

Figure 1.1 Reaction Coordinate Diagrams [Ref.8]

TABLE III

Reactions for $F+H_2$ Laser [Ref. 8]

Reaction	Overall Rate Coefficients[a]		Distribution Constants a(v)			
	Forward	Backward	v=0	1	2	3
$F+H_2 \rightleftarrows HF(v)+H$	$k=1.62\times10^{14}e_1$	$k_b=0$	0.056	0.111	0.555	0.278
$HF(v)+HF \rightleftarrows HF(v-1)+HF$	$k_{HF}=6\times10^{16}T^{-1.43}$	$k_b=0$	0	0.167	0.333	0.500
$HF(v)+H_2(0) \rightleftarrows HF(v-1)+H_2(1)$	$k_{H_2}=8.3\times10^{5}T^{2.2}e_2$	$k_b=0$	0	0.965	0.035	0
$HF(v)+F \rightleftarrows HF(v-1)+F$	$k_F=5.4\times10^{9}T^{1.3}$	$k_b=0$	0	0.167	0.333	0.500
$2HF(v) \rightleftarrows HF(v-1)+HF(v+1)$	$k_{fHF}(T)$	$k_b=0$	0	$a_f(1)$	$a_f(2)$	0
$2HF(v) \rightleftarrows HF(v-1)+HF(v+1)$	$k_f=0$	$k_{bHF}(T)$	0	$a_b(1)$	$a_b(2)$	0

[a] All rate coefficients are in cm^3/mole-sec, and R = 1.987 cal/mole - °K. Here $e_1 = \exp[-1600/RT]$ and $e_2 = \exp[-562/RT]$.

REPRODUCED AT GOVERNMENT EXPENSE

REPRODUCED AT GOVERNMENT EXPENSE

Table II
Electrical Discharge Driven Lasers (cont'd.) [Ref. 2]

Glass, 1971, (50)	$F + H_2 \rightarrow HF$ $F + D_2 \rightarrow DF$, Near sonic mixing laser, F_2 + He	21 MHz rf discharge, 50-100 W	HF: 300	2-1, 1-0	1% MgF_2 flat coupler	41	1.0	He = 2.6 H_2 = 0.1 D_2 = 0.1 F_2 = 0.3	0.5 × 3.0	Multi-slit nozzle, detailed gain measurements
			DF: 120	3-2	5% MgF_2 flat coupler					
Stephen and Cool, 1971, (49)	$F + H_2 \rightarrow HF$ $F + D_2 \rightarrow DF$, Near sonic mixing laser, SF_6 + He	27 MHz rf discharge, 2500 W	HF: 1 500	2-1, 1-0	5% coupler	180	9.8	He = 11 H_2 = 0.78 SF_6 = 2.1	3.0 × 4.5	Single slit, sonic wall injection
			DF: 500	3-2 to 1-0	2% coupler	100	4.7	He = 11 D_2 = 1.4 SF_6 = 0.26		
Rosen et al., 1973, (42)	$F + H_2 \rightarrow HF$ $F + HI \rightarrow HF$ $F + CH_4 \rightarrow HF$ $F + HBr \rightarrow HF$ $F + HCl \rightarrow HF$ $Cl + HI \rightarrow HCl$, Subsonic mixing laser, F_2, Cl_2 + He	2450 MHz microwave discharge, 1000 W	7 500 2 300 1 500 2 000 1 700 1 650 100	3-2 to 1-0 5-4 to 1-0 3-2 to 1-0 4-3 to 1-0 3-2 to 1-0 4-3 to 1-0 2-1 to 1-0	10% 10% 5% 5% 2% 5% 0.5% couplers	840	6.0	He / H_2, HI / F_2, Cl_2: 64 / 2.9 / 0.60 67 / 0.39 / 0.59 67 / 0.89 / 0.49 70 / 0.34 / 0.49 70 / 0.53 / 0.86 56 / 0.73 / 2.3 70 / 1.5 / 2.1	0.7 × 10.0	Multi-tube injector, detailed spectroscopy of all reactions, chemiluminescence studied
Glass and Landford, 1973, (45)	$F + H_2 \rightarrow HF$, Subsonic mixing laser, F_2 + He	8 MHz rf discharge, 1300 W	10 000	3-2 to 1-0	25% MgF_2 flat coupler	94.6	3.0	He = 20 H_2 = 2 F_2 = 2	1.0 × 14.0	Multi-slit nozzle
Hinchen, 1974, (46)	$F + H_2 \rightarrow HF$ $F + D_2 \rightarrow DF$, Subsonic mixing laser, SF_6 + He	High voltage dc discharge, 1300 W	HF: 1 300	2-1, 1-0	25% coupler	14	10-15	He = 5.8 H_2 = 0.8 O_2 = 0.5 SF_6 = 2.4	0.3 × 10.0	Very stable single mode output, gain line measurements
			DF:	3-2 to 1-0	Single hole	14	10-15	He = 2.5 D_2 = 1.0 SF_6 = 3.0		

TABLE II

Electrical Discharge Driven Lasers [Ref. 2]

Name, Year, Reference	Reaction, Device, Main Flow	Discharge Type	Maximum Power (mW)	Laser Transitions	Coupling Mode	Pump Capacity (l/sec)	Cavity Pressure (Torr)	Flow Rates (mmol/sec)	Channel Cross Section (cm)	Remarks
Naegeli and Ultee, 1970, (43)	Cl + HI → HCl_v Subsonic mixing laser, Cl_2 + He	High voltage + microwave 60 Hz + 2450 MHz	0.47	2-1	Single hole	235	2	Not measured	0.5 × 15	
Cool et al., 1970, (41)	F + H_2 → HF H + F_2 → HF F + HI → HF F + D_2 → DF D + F_2 → DF F + DI → DF H + Cl_2 → HCl Cl + HI → HCl H + HBr → HBr Br + HI → HBr, Near sonic longitudinal mixing laser, F_2, Cl_2, Br_2, H_2, D_2, He	27 MHz rf discharge	53 50 4 83 80 2 1 12 None None	2-1 2-1 3-2, 2-1 3-2, 2-1 3-2 3-2 1-0 2-1, 1-0 --- ---	5% 5% 0.5% 2% 2% 0.5% 0.5% 2% -- -- couplers	200	24 27 17 21 32 19 45 21 -- --	He, H_2,D_2, F_2,Cl_2 18, 0.18, 0.10 21, 0.28, 0.22 11, 0.06, 0.11 16, 0.18, 0.17 25, 0.37, 0.45 14, 0.12, 0.13 37, 2.00, 0.28 18, 0.05, 0.04 ---- ----		Narrow bore tube, cavity axis along flow axis, very detailed study
Hinchen and Banas, 1970, (51)	F + H_2 → HF F + D_2 → DF, Subsonic mixing laser, SF_6 + N_2, He	High voltage dc discharge, 1500-6000 W	HF: 5 500 DF: 3 000	2-1, 1-0 3-2 to 1-0	Single hole	235	5.9	He = 10 N_2 = 20 H_2 = 3 SF_6 = 3-20	1.25 × 30	
Bussoh et al., 1970, (47)	F + H_2 → HF F + D_2 → DF, Subsonic premixed, SF_6 + H_2, D_2 + He	High voltage dc discharge, transverse to flow, magnetically stabilized	HF: 800 DF: 30	2-1, 1-0 3-2, 2-1	20% coupler 2.5% coupler	>300	8.5	He = 13.6 H_2 = 2.6 D_2 = 2.6 SF_6 = 8.5	1.6 × 3.0	
Glaze et al., 1971, (44)	Cl + HI → HCl_v Near sonic mixing laser, F_2 + He	21 MHz rf discharge, 50-100 W	70	2-1, 1-0	4.6% MgF_2 flat coupler	41	3.0	He = 3.0 Cl_2 = 0.2 HI = 0.25	0.5 × 3.0	Multi-slit nozzle, gain measurements

REPRODUCED AT GOVERNMENT EXPENSE

TABLE I

Thermally Driven Lasers [Ref. 2]

Name, Year, Reference	Reaction, Main Flow, Device	Maximum Flow (g/sec)	Maximum Power (W)	Mirror Size, Cavity Type, Output Mode	Nozzle Dimensions (cm)	Chemical Efficiency (%)	Specific Power (W/g/sec)	Power Input (kW)	Pressure		Plenum Temp (K)
									Cavity (Torr)	Plenum (atm)	
Gross et al., 1969, (7)	$F_2 + H_2$, $F_2O + H_2 + Ar$, Shock tube detonation wave laser	(Shock speed 1.8-2.0 mm/μsec)	10 (peak power)	2.5 cm Ø, Stable, Single hole transverse	2.5 × 17.6 (cavity)			None	18 (p_2)		2000 (T_2)
Airey and McKay, 1969, (3)	F + HCl, F_2 + Ar, Supersonic shock tube driven		8×10^{-4}	1.0 cm Ø, Stable, Single hole transverse	1.0 × 15 (1 slit)			None	8-19	0.7-2.3	1050
Spencer et al., 1969, (5)	F + H_2, $SF_6 + N_2$, Supersonic arc heater	N_2 = 15 H_2 = 2 SF_6 = 0.54	1	4.5 cm Ø, Stable, Single hole transverse	0.95 × 17.6 (1 slit)		0.057	20	10	3	2000
1970, (15)	F + H_2, D_2, $SF_6 + N_2$, Supersonic arc heater	N_2 = 7.4 H_2 = 1.0 D_2 = 1.6 SF_2 = 1.7	HF: 600 DF: 450	4.5 cm Ø, Stable, Multi-hole transverse	0.95 × 17.6 (36 slits)	12	60	30	4.7	1.7	2300
1973, (23)	F + H_2, D_2, SF_6 + He + O_2, Supersonic arc heater	He = 6.9 H_2 = 1.0 O_2 = 0.9 SF_6 = 3.3	2 000	9.6 × 9.6 cm, Stable, Closed cavity transverse	1.27 × 17.6 (36 slits)	9.8	245	35-50	4.5	1.3	2000
Giedt 1973, (31)	F + H_2, D_2, F_2 + He, Supersonic arc heater	He = 20 H_2 = 11 F_2 = 15	12 360	9.6 × 9.6 cm, Stable, Closed cavity transverse	1.9 × 22.9 (36 slits)	12	271	336	2.3	6.1	1400
Morsell 1971, (32)	F + H_2, F_2 + He, Supersonic resistive heater	He = 2.0 H_2 = 0.33 F_2 = 1.3	148	5.0 cm Ø, Stable, Germanium flat transverse	1 × 15 (1 slit)	2.5	40	2.4	4.1	0.30	2020
Meinzer et al., 1970, (38)	F + D_2, H_2, F_2 + He, Supersonic combustion heater	F_2 = 0.38 D_2 = 0.04 H_2 = 0.02 (combustor)	10	Stable, Single hole transverse	1 × 10 (1 slit)			None	3.8	5	2200
Shirley et al., 1971, (36)	F + H_2, D_2, F_2 + He + NO, Subsonic driver by chemical reaction	He = 50-150 H_2 = 5 F_2 = 20 NO = 1	7.2	Stable, Germanium flat transverse	1 × 15 (1 slit)	0.5		None	8.0		400-700
Blaszuk et al., 1973, (39)	F + D_2, H_2, F_2 + He, Supersonic combustion heater	37 (total)	HF: 3 000 DF: 1 740	Stable, Silicon flat, transverse Unstable, transverse	1.05 × 45.5 (matrix of 3600 holes) 1.05 × 45.5 (matrix of 3600 holes)		162 52	None None	7.5 8.2	1.1 1.5	1300 1300

REPRODUCED AT GOVERNMENT EXPENSE

REPRODUCED AT GOVERNMENT EXPENSE

$$\Phi_{rad} = k\rho^2 n_F^0 n_{H_2}^0 \Big[(m_1 - 1)(1-\xi)(1-k_1\xi) - \left(\frac{\xi}{m_3} + m_5\alpha\right)(1-k_1\xi)\overline{k}_H - k_1 \frac{m_2\xi}{m_3} + m_4\alpha[\overline{k}_{HF}\xi + (1-\xi)\overline{k}_F] \Big] . \quad \text{(eqn 1.17)}$$

But we want to know the total output power available. We know the circulating power per unit volume inside the cavity is given as

$$gI_i = hcN\omega\Phi_{rad} . \quad \text{(eqn 1.18)}$$

The total power per unit mole-density is then found by integration of ϕ over the entire flow direction and is given as

$$P = hcN\omega A\int_0^{x_f} \Phi_{rad} dx , \quad \text{(eqn 1.19)}$$

where

A = cross sectional area of flow,

ω= wavenumber of the laser transition,

h= Planck's constant,

N= Avogadro's number,

P= units of watts/mole-volume.

It must be said again that this is only a qualitative modeling of the HF/DF laser and did not assume any mixing conditions. In the actual HF/DF laser the mixing processes are as important as the kinetic processes. Figure 1.3 shows the difference in the mixed and premixed cases where the gain zone is shown as a fun on of downstream distance.

REPRODUCED AT GOVERNMENT EXPENSE

Now that we have the equation for the net production of excited states we need to determine the number of moles of each specific gas in the gas flow; n_F, n_{H_2}, n_{HF}, and n_H. The first equation of figure 1.1 gives the changes in fluorine and hydrogen density during the chemical reaction.

$$V\frac{\partial n_F}{\partial x} = -V\frac{\partial n_H}{\partial x} = -k\rho n_F n_{H_2} \quad \text{(eqn 1.13)}$$

Utilizing the above equation and the conservation of mass (number of atoms) we can solve for the number of moles of each species in the gas flow [Ref. 8]. The zero in the superscript means the number of moles of a species at x=0. Assume that $n^0_{HF}=0$ and $n^0_H=0$. From the conservation of mass we have $n_H+n_{HF}+2n_{H_2}=n^0_H+n^0_{HF}+2n^0_{H_2}$, $n_F+n_H=n^0_F+n^0_H$, and $n_F+n_{HF}=n^0_F+n^0_{HF}$.

$$\frac{n_F}{n^0_F} = \frac{[1-(n^0_F/n^0_{H_2})]\exp[-k\rho(n^0_{H_2} - n^0_F)x/V]}{[1-(n^0_F/n^0_{H_2})]\exp[-k\rho(n^0_{H_2}-n^0_F)x/V]} \quad \text{(eqn 1.14)}$$

$$\frac{n_{HF}}{n^0_F} = \xi = \frac{1-\exp[k\rho(n^0_{H_2}-n^0_F)x/V]}{1-(n^0_F/n^0_{H_2})\exp[-k\rho(n^0_{H_2}-n^0_F)x/V]} \quad \text{(eqn 1.15)}$$

$$\frac{n_{H_2}}{n^0_F} = \frac{n_{H_2}}{n^0_F} \quad \frac{1-\exp[-k\rho(n^0_{H_2}-n^0_F)x/V]}{1-(n^0_F/n^0_{H_2})\exp[-k\rho(n^0_{H_2}-n^0_F)x/V]} \quad \text{(eqn 1.16)}$$

Using these three equations along with equations 1.6, 1.11, and 1.12 we can solve for A_1 and A_2 from which we can find the production rate of population in the V state by radiative means in the transition V+1 to V designated $\Phi_{rad} = \Phi(V)$.

REPRODUCED AT GOVERNMENT EXPENSE

and vibrational energy exchanges. Table III shows the overall rate coefficients, k, and distribution constants, a(V), for specified chemical reactions.

From [Ref. 8] we can define the net production of excited states, (V), as:

$$\lambda(V) = \rho^2 k a(V) n_F n_{H_2}$$
$$+ k_{HF} n_{HF} [a_{HF} - (V+1) n(V+1) - a_{HF}(V) n(V)]$$
$$+ k_F n_F [a_F(V+1) n(V+1) - a_F(V) n(V)] \qquad \text{(eqn 1.12)}$$
$$+ k_{H_2} n_{H_2} [a_{H_2}(V+1) n(V+1) - a_{H_2}(V) n(V)]$$
$$+ f(k_{f_{HF}}, k_{b_{HF}})$$
$$V=0,1,2$$

A detailed developement of equation 1.12 is given in reference 9. The distribution constants, a(V), fix the rate of production for each vibrational level while k is the reaction constant. The product ka(V) is the rate into a particular vibrational level V [Ref. 8]. Equation 1.12 contains terms representing the production of vibrationally excited HF, the V-T deactivation of HF by HF, deactivation due to F, deactivation due to H_2, and the V-V transfer of energy between HF molecules in collisions. A V-T reaction is a reaction in which the vibrational kinetic energy of the reactants is converted into translational kinetic energy of the colliding particles [Ref. 10]. Reference 10 shows the equation that is followed for the V-T reaction.

REPRODUCED AT GOVERNMENT EXPENSE

ρ = the density of the species.

$\Delta J=-1$ (emission) for a P-branch transition.
Solving this set of linear equations 1.7 and 1.8 we find n(V) to be [Ref. 8]

$$n(V) = \left[\frac{1-\exp(-2J\delta)}{1-\exp(-2J\delta(V_f+1))}\right]\exp(-2J\delta V n_{total})$$
$$+\left[\frac{g}{g_r}\left[\frac{\exp[(J^2-J)\delta]}{J[1-\exp(-2J\delta)][1-\exp(-2J\delta(V_f+1))]}\right]\right]$$
$$* \left[[1-\exp(-2J\delta V)][1-\exp(-2J\delta(V_f+1))]\right.$$
$$-[V_f\exp(-2J\delta V)][1-\exp(-2J\delta)] \qquad \text{(eqn 1.9)}$$
$$\left.+[\exp(-2J\delta(V+1))][1-\exp(-2J\delta V_f)]\right].$$

$$V=0,1,\ldots V_f.$$

where

$$\delta = T_r/T.$$

$$n_{HF} = \sum_{V=0}^{V_f} n(V)$$

is the total number of HF moles per unit mass.
Taking the derivative of equation 1.9 and combining it with equation 1.7 we can solve for A_1.

$$\frac{\partial n(V)}{\partial x} = \left[\frac{1-\exp(-2J\delta)}{1-\exp(-2J\delta(V_f+1))}\right]\exp(-2J\delta)\frac{\partial n_{HF}}{\partial x}. \qquad \text{(eqn 1.10)}$$

$$A1=\rho v\left[\frac{1-\exp(-2J\delta)}{1-\exp(-2J\delta(V_f+1))}\right]\frac{\partial n_{HF}}{\partial x}\sum_{V=0}^{(V_f-1)}(V_f-V)\exp(-2J\delta V) \qquad \text{(eqn 1.11)}$$

where $\frac{\partial n_{HF}}{\partial x}$ is determined from the chemical kinetics of the reaction as well as from A_2 which represents the chemical

REPRODUCED AT GOVERNMENT EXPENSE

In order to find A_1 and A_2 we must examine one of the two limiting cases involving the mixing of the two gases hydrogen and fluorine. Once these atomic species are mixed the reaction starts immediately with the overall rate of reaction being dependent upon the chemical reaction rate and the rate of mixing [Ref. 8]. The limiting cases are fast mixing or slow mixing of the compounds relative to the reaction rate. The fast mixing or "premixed" case is the simpler of the two and will be examined further. The production of HF in this case is dependent upon and limited by the chemical reaction rate. A detailed description of the "premixed" situation is modeled in reference 9.

In a transverse flow, steady state oscillator the gain is given by the relationship [Ref. 8]

$$R_1 R_2 \exp[2Lg(V,J)] = 1. \qquad \text{(eqn 1.7)}$$

where g(V,J) is the gain coefficient per unit laser length, L. Equation 1.7 is the threshold condition and must be satisfied in order for lasing (steady state oscillation) to occur [Ref. 10]. The reflectivities of the mirrors in the cavity are given as R_1 and R_2. The gain coefficient for a P-branch vibrational-rotational transition is

$$g(v,J) = g_r J \exp[-J(J-1)T_r/T] * [n(V+1) - n(V)\exp(-2JT_r/T)] \qquad \text{(eqn 1.8)}$$

where

T = the translational temperature,

T_r = the rotational temperature,

J = the rotational quantum number of the upper state,

$g_r = [C\rho T/(T_r)^{3/2}]$,

C = the dipole matrix element.

REPRODUCED AT GOVERNMENT EXPENSE

The population of each vibrational state, $n(V)$, can be written as the number of moles of HF in a particular state [Ref. 8].

$$\rho v \frac{\partial n(0)}{\partial x} = \lambda(0) + \Phi(0)$$

$$\rho v \frac{\partial n(1)}{\partial x} = \lambda(1) + \Phi(1) - \Phi(0)$$

(eqn 1.3)

$$\rho v \frac{\partial n(V_f)}{\partial x} = \lambda(V_f) - \Phi(V_f - 1)$$

where

ρ = density

v = velocity of the flowing system

V_f = highest vibrational level considered

$\lambda(V)$ = production rate of the state V by chemical and vibrational exchange

$\Phi(V)$ = production rate of the state V by radiation in the transition V+1 to V

Solving for Φ and summing the results we get for the production rates:

$$\Phi = \sum_{V=0}^{(V_f-1)} \Phi(V) = A_1 - A_2 \quad \text{(eqn 1.4)}$$

where:

$$A_1 = \rho v \sum_{V=0}^{(V_f-1)} (V_f - V) \frac{\partial n(V)}{\partial x}, \quad \text{(eqn 1.5)}$$

$$A_2 = \sum_{V=0}^{(V_f-1)} (V_f - V) \lambda(V) \quad \text{(eqn 1.6)}$$

produced by electrical dissociation of Sulfur Hexafluoride (SF_6) to provide the free fluorine atoms necessary for excitation with hydrogen.

The type of reaction in which a product is formed in an excited state is of major concern. The population of the product state may be inverted with respect to some lower state thus allowing a lasing action. In the HF/DF laser hydrogen, or deuterium, reacts with the fluorine and produces a population inversion in some vibrational levels of the HF or DF molecules. Our primary concern is with the "cold" reaction where we have a heat of reaction of h= -31.7 kcal/mole. The basic reaction is [Ref. 7]

$$F + H_2 = H + HF^* \qquad \text{(eqn 1.1)}$$

for the HF laser and is

$$F + D_2 = H + DF^* \qquad \text{(eqn 1.2)}$$

for the DF laser. The reaction diagrams are shown as figure 1.1. Any of the V=0,1,2,3 in HF and V=0,1,2,3,4 in the DF vibrational states can be generated by the chemical reaction specified in equations 1.1 and 1.2.

More molecules will be found in the higher vibrational states than in the lower states, producing a population inversion. The inversion occurs because of the differences in the reaction rates between the vibrational states. Population densities for the different vibrational states are given in figure 1.2 [Ref. 7]. The population inversion of n , n_2, and n_3 can be seen within approximately 1 cm downstream of the flame. This distance is very critical when aligning the laser cavity for resonance. The alignment of the beam through the cavity must be within 0.8 mm of the active lasing zone in the flame for lasing to occur.

II. LASER DESIGN

A. INTRODUCTION

The HF/DF laser at NPS is a small-scale continuous wave chemical laser. It was procured from the Aerospace Corporation in June 1976 and installed in Spanagel Hall room 609 in July 1976. The entire system consists of a laser bench which supports the actual laser and houses the gas flow rate gauges and ballast resistors. Its support systems include

1. gas supply system,
2. water cooling system,
3. dc power supply,
4. vacuum system.
5. scrubber system
6. detector system

The entire laser system is shown schematically in figure 2.1 Most of the subsystems listed are discussed in reference 6, with the remaining ones being discussed later in this presentation. Step by step guidelines f the operation of the laser system will be discussed and outlined in the following chapter. Figure 2.2 shows the HF/DF laser flow channel. For convenience this has been sectioned into five regions [Ref. 3]

1. discharge region,
2. inlet region,
3. lasing zone,
4. heat exchanger region,
5. exhaust region.

A detailed discussion of each of these regions follows in the next section of this chapter.

B. REGIONS OF THE HF/DF LASER

1. Discharge Region

The discharge region consists of eight 1/16 inch diameter by 6 inch long Nickel discharge anodes supported inside a pyrex discharge tube with an inner diameter of 1.26 inches and a wall thickness of 0.062 inches. The pyrex discharge tube is surrounded by a lucite tube acting as a water jacket with an inner diameter of 1.75 inches and a wall thickness of 0.25 inches. Both of these tubes are nominally used in two lengths, 12 and 24 inches, with 10 and 20 kV power supplies, respectively [Ref. 3]. There are also interface connections for SF_6, He, and O_2 inlets, water jacket cooling water inlet and outlet, and power supply anodes and cathode.

SF_6, He, and O_2 are premixed at 100 psi and injected into the discharge region upstream of the 8 Nickel discharge anodes in order to provide the free fluorine radicals necessary to generate vibrationally excited HF or DF molecules. Spencer, Beggs, and Mirels [Ref. 3] found that the discharge uniformity at the anodes was highly dependent upon the uniformity of the flow of gases at the tips of the Nickel anodes. They therefore made the gas injection as uniform as possible into the discharge region. SF_6 is our source for the free fluorine radicals and is dissociated by a high voltage DC discharge. The dissociation of SF_6 is a very complicated process with many different types of reactions occurring. Equation 2.1 is the least likely reaction to occur. It is placed in the text to show an initiation technique for the production of the free fluorine radicals.

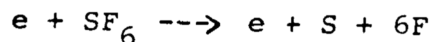

$$e + SF_6 \longrightarrow e + S + 6F$$

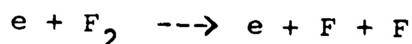

$$e + F_2 \longrightarrow e + F + F \qquad \text{(eqn 2.1)}$$

Experimental work showed that SF_6 was not b‹ ıng completely dissociated at the maximum power point which implied that the power could be increased if complete dissociation of SF_6 were achieved [Ref. 11]. Addition of O_2 into the discharge region increased the heat of combustion which led to an increase of the concentration of the free fluorine radicals by following the reaction

$$SF_4 + O_2 \longrightarrow SO_2F_2 + 2F \qquad \text{(eqn 2.2)}$$

The effect on laser power and efficiency of varying the f ›w rates of O_2 and SF_6 is discussed in reference 11. The addition of O_2 also cuts down on the sulfur deposits on the discharge tube.

The addition of He to the discharge flow acts to stabilize the discharge by reducing the required discharge voltage and reduces the gas temperature of the discharge flow by acting as a thermal diluent.

The power supply is a Hipotronics DC power supply that applies a voltage to the mixed gases in order to dissociate the SF_6 so that free fluorine radicals are available for interaction with hydrogen to form the excited HF . The power supply, model number 825-1a, has input specifications of 440 V ac, 3 Φ, 40 Amp, and 60 Hz with output specifications of 0-25 kV dc at 1 Amp. The output is continuously adjustable which allows for proper ionization of the discharge flow. A diagram of the hipotronics DC power supply is shown in figure 2.3.

The actual discharge takes place along the centerline of the pyrex discharge tube starting from the 8 nickel anodes and ending on a copper cathode. The hot flow of gases passes from the discharge region of circular cross-section into the inlet region of channel (rectangular) cross-section of approximately 10cm by 0.3cm.

2. Inlet Region

The temperature of the hot gas flow at the front of the inlet region is approximately 700 degrees celsius [Ref. 3]. The hot gas flow carries the free fluorine into the inlet region. The H_2 is then injected into the flow from the top and the bottom of the flow channel through 80 holes each with a diameter of 0.0135 inches. The holes are situated such that 40 are at the top of the channel and 40 are at the bottom of the channel transverse to the direction of gas flow. Just downstream of the H_2 injection ports the H_2 mixes with the free F in the lasing zone.

3. Lasing Zone

In the lasing zone the H_2 mixes with the F to produce the excited HF^* for lasing. At this point in the flow field the temperature has decreased to a nominal temperature of 400 degrees celsius. The lasing zone is only 0.8 mm wide so that alignment of the cavity is very critical. The alignment procedure for multiline operation is given in appendix C.

4. Heat Exchanger Region

The remaining portion of the Amsulf block cavity acts as a heat exchanger to reduce the temperature of the gas flow to a nominal temperature of 200 degrees celsius. The flow cross-section is also changed from the square channel geometry back to the circular geometry of the exhaust piping system for ease of exhausting the hot gas flow.

5. Exhaust Region

The exhaust region consists of piping connecting a scrubber system with a vacuum pump system. The hot gas flow

exits the heat exchanger region 1 flows into a scrubber system consisting of yered scre d drawers of soda lime As the gas flow passes through the drawers the soda lime neutralizes the noxious nature of the gases. A detailed description of the scrubber system is given in reference 6. The gas flow then is exhausted to atmosphere via the water cooled vacuum pump system which is also described in detail in reference 6.

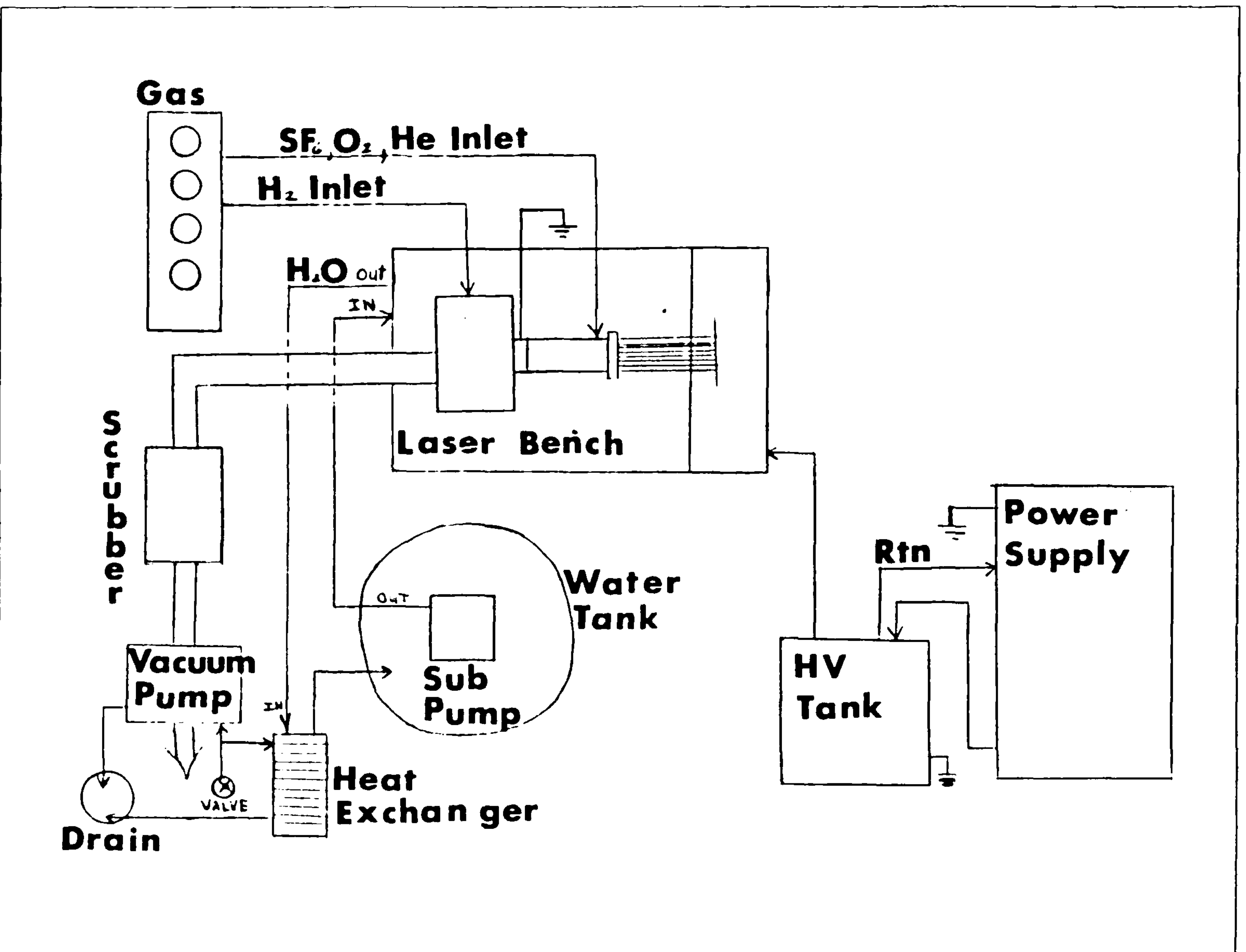

Figure 2.1 The NPS HF/DF Laser System

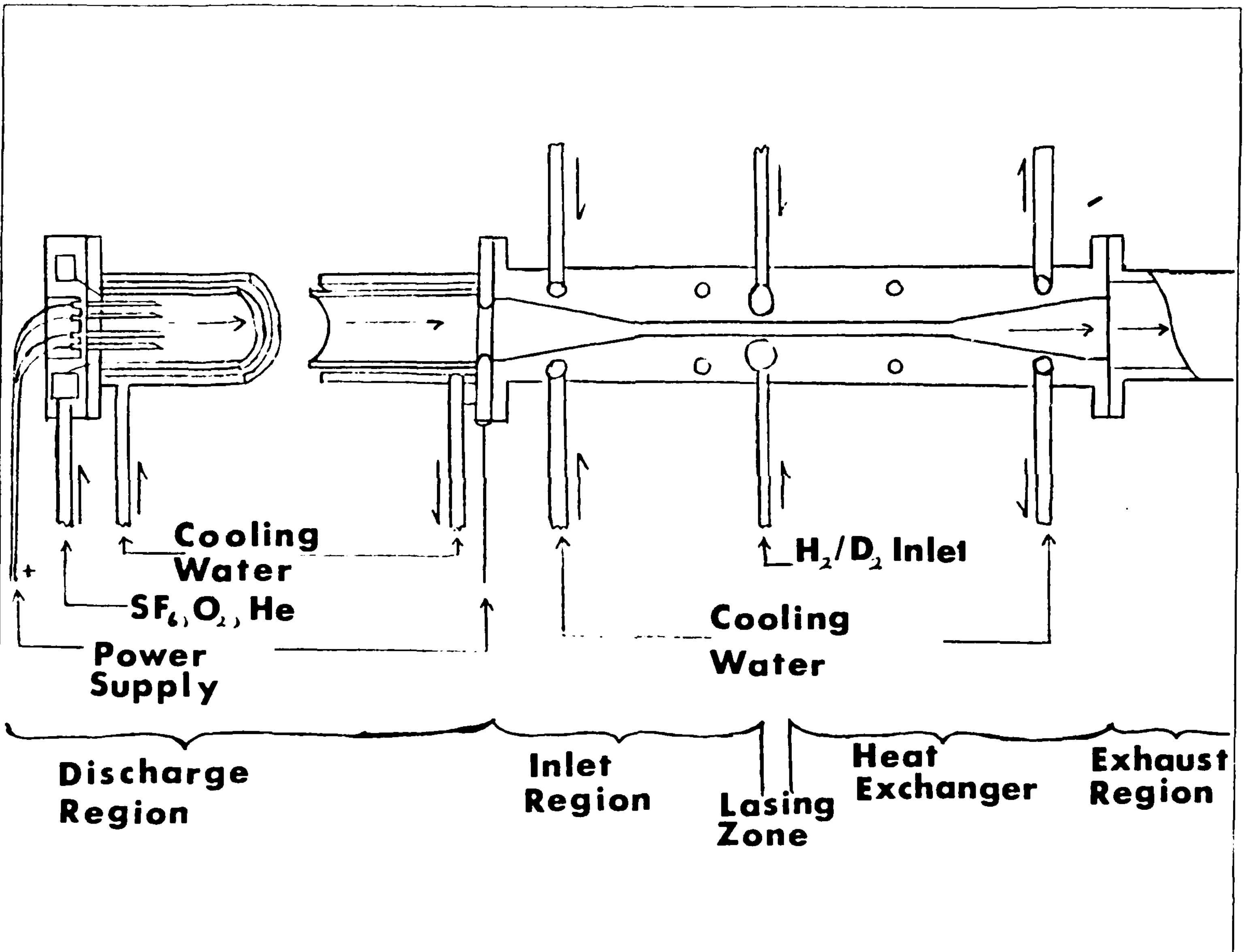

Figure 2.2 HF/DF Laser Regions [Ref.2]

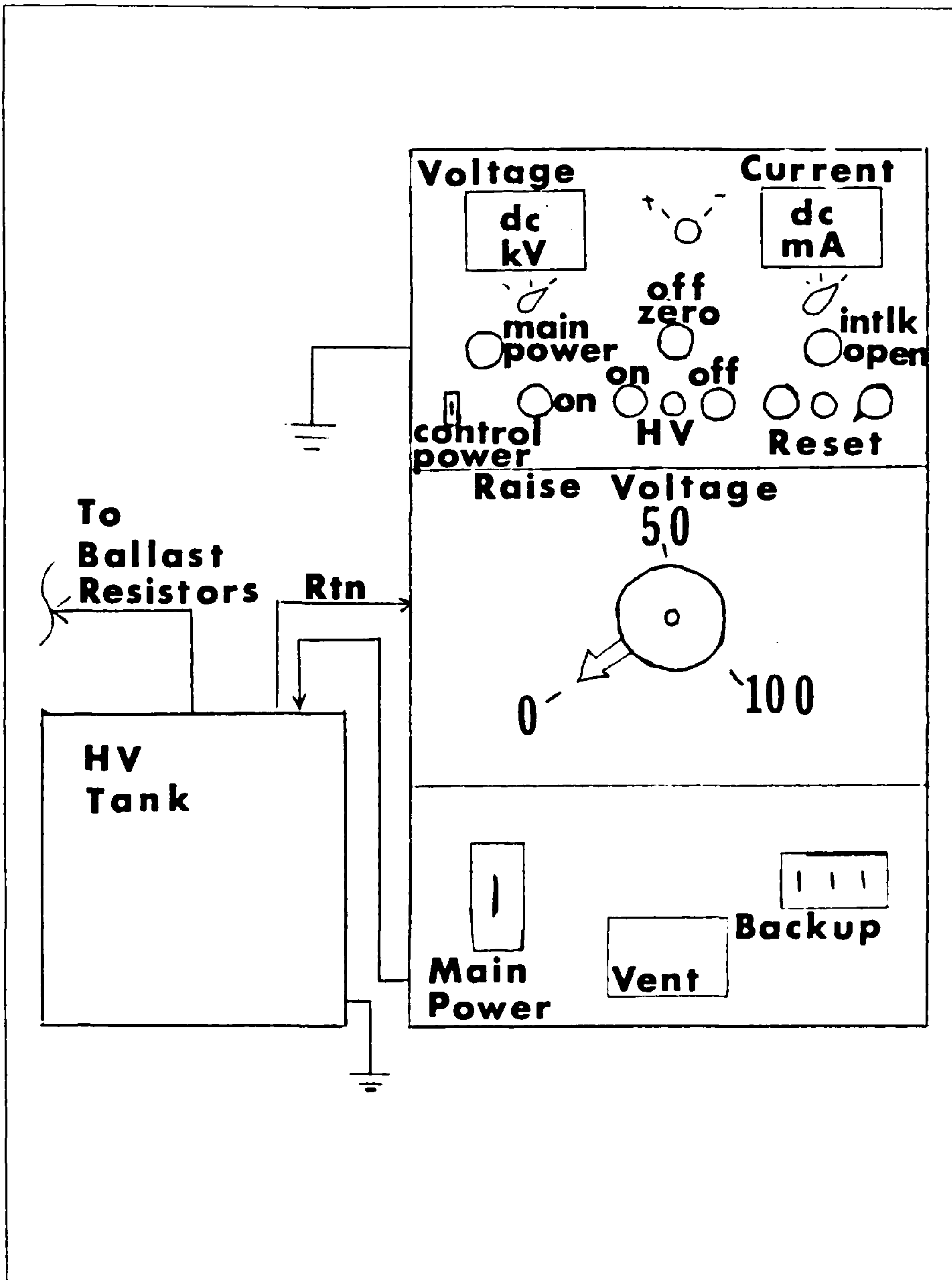

Figure 2.3 Hipotronics Power Supply

III. OPERATING CHARACTERISTICS

A. INTRODUCTION TO HF OPERATION

The HF/DF laser at NPS can presently be operated in four different configurations as listed below:

1. HF multiline operation,
2. HF single line operation,
3. DF multiline operation,
4. DF single line operation.

Of the four listed configurations only the HF multiline operation will be discussed in any detail. The reasoning for this is to show that after seven years of non-operation of the laser the basic parameters established in 1977 for the operation of this laser have been re-established.

After discussing the operating characteristics of the HF multiline laser the reflectivity for the CW laser radiation of target materials will be reported and discussed as well as the potential design and subsequent operation of a system that will pulse the HF laser as well as increase the output power for future use with laser target interaction.

B. HF MULTILINE OPERATION

Data was obtained for the variation of power with the change in flow rate of each of the gases utilized with the HF/DF laser as well as with the change in input dissociation voltage. The results were in agreement with previously reported measurements and will be discussed further.

The optimum flow rate of each of the gases was previously determined to be:

SF_6 = 18 steel ball,
O_2 = 100 steel ball,
H_2 = 30 steel ball,
He = 45 steel ball,
Input Voltage = 16.5 kV,

where these steel ball readings refer to the scale locations of the steel ball indicator in the flow meter. For the actual flow rates in grams/second see Table IV . Power output fluctuated between 1.00 and 1.60 Watts once these optimum conditions had been met. Further measurements showed that because of the new power supply that had been installed the input voltage for dissociation could be increased which changed the optimum operating conditions. The new optimum flow rates were found to be:

SF_6 = 21 steel ball,
O_2 = 75 steel ball,
H_2 = 31 steel ball,
He = 65 steel ball,
Input Voltage = 19 kV.

Power output fluctuated between 2.00 and 2.60 Watts once these optimum conditions had been met. By utilizing the higher voltage with the changed flow rates more SF_6 could be dissociated thus forming more free fluorine radicals that could combine with the hydrogen to form excited HF^*. This increased the maximum power output for the 95 percent output coupling mirror from 1.60 to 2.60 Watts which is approximately a 62 percent increase in output power.

Power variation with the change in SF_6 flow rate is plotted in figure 3.1. As the flow of SF_6 was increased the power continued to increase until an optimum flow was achieved. This flow was a steel ball reading of 21 and corresponds to the flow rate at which SF_6 is balanced with O_2 for maximum dissociation of SF_6 . It is highly unlikely that the SF_6 will completely dissociate. We can also see from figure 3.1 that increasing the flow beyond a rate of 21 the power begins to decrease. This decrease in power is due to the increase in collisional deactivation because of the increase in density of the excited HF^* molecules.

Power variation with the change in H_2 flow rate is plotted in figure 3.2. The effects of the increase of H_2 flow are similar to those discussed above for SF_6. As the H_2 flow rate increased the power increased and reached a peak at the optimum flow of H_2 at a steel ball reading of 31. This optimum flow was found to be the flow at which H_2 flow was balanced to the flows of SF_6 and O_2. As the flow of H_2 was increased beyond the optimum flow point the power began to fall because of collisional deactivation.

Power variation with the change in O_2 flow rate is plotted in figure 3.3. The interesting point about this figure is that at a zero flow of O_2 lasing occurred at a power out of approximately 0.1 watts. As the flow of O_2 was increased the power abruptly increased by a factor of 16 and continued to increase an additional factor of 5 until the optimum flow was obtained at a steel ball reading of 75. The addition of O_2 assists in the oxidation of the fuel flow and increases the dissociation of SF_6 by increasing the heat of combustion as given by equation 2.2.

Power variation with the change in He flow rate is plotted in figure 3.4. From the figure we see, like O_2, that He is an auxilliary gas which maximizes the density of the excited HF^* in the lasing zone. The excited HF^* is buffered from collisions with other excited HF^* by the addition of He, thus avoiding a loss of excited HF^*. Essentially, the collisional self-relaxation of the excited HF^* is prevented from occurring until after it has passed the gain zone(lasing zone) of the cavity. The interesting point about this figure is the twin peaks of power occurring at steel ball readings of 40 and 65 respectively. All previous experimentation has not shown this type of result so further data was taken. The optimum He flow was found to be 65 in conjunction with the previous stated flows of SF_6, H_2, and O_2. Power output was nominally 0.4 Watts higher than when

operating at a flow of 40 for long periods of operation. Based on these findings the conclusion was made that a proper settling time for the laser must be allowed when and after changes in flow have occurred. In addition, when gas in the bottles is below 250 psi they should be changed in order to prevent any unwanted fluctuations in flow.

Power variation with change in input voltage is plotted in figure 3.5. From the figure we can see that the increase in input voltage does increase the power output of the laser. The peak power output occurred at 19 kV. As the input voltage continued to increase the power out began to fall. The increase in power was obtained because the increase in voltage allowed for an increase in dissociation of the SF_6. The power began to fall off because the increase in free fluorine radicals increased the density of excited HF molecules thus increasing the possibility of collisional deactivation. The presence of ground state HF will decrease the gain, but gain is proportional $n_{HF^*(V+1)} - n_{HF^*(V)}$.

C. TARGET REFLECTIVITY/ABSORPTIVITY

Target reflectivity/absorptivity measurements were taken utilizing the HF/DF laser. The target material chosen was a polished Silicon wafer with the Silicon crystals doped with Boron. There were two reasons for using these wafers as target materials:

1. Silicon is the basis material for many commercial and military electro-optical sensing systems.
2. The same target material was used by Chenoweth and Johnson in target damage interaction measurements. Future target damage measurements with the HF/DF laser could be compared to the measurements obtained by Chenoweth and Johnson which are described in reference 12.

The basic experimental setup is shown in figure 3.6. The output power was measured over a number of readings in order to obtain an average power output that would be interacting with the target material. This average power output was found to be 2.26 Watts. The output power was then split by a CaF_2 beamsplitter prior to target interaction. The measurements obtained showed that the power split from the main output beam was 0.4537 Watts. The average power incident on the target was measured as 0.4600 Watts.

The target material was placed into a lens holder and mounted upon a brass angle indicator so that measurements of power reflectivity from the target could be taken as a function of target angle relative to the incident laser beam. Measurements of the specularly reflected power were taken in five degree increments over a range of forty degrees starting with 25 degrees and ending with 65 degrees. Figure 3.7 shows the effect of target angle on reflected power. As the angle increased from 25 to 60 degrees the power reflected increased. At the target angle of 65 degrees the reflected power decreased substantially. This decrease in reflected power is thought to be due to the misalignment of the power detector measuring the reflected power. Figure 3.8 shows the power absorbed as a function of target angle. From this figure we can see that as the angle was increased the power absorbed by the target decreased.

The laser beam was positioned so that it was normal to the target. The target was then rotated through the range of angles descibed above. As the target angle was changed the reflected power specular angle changed; therefore the power detector had to be moved to find the maximum power reflected. This was not an easy task and took considerable time to move the detector to the optimum power measurement position.

The most interesting and important finding of these measurements was that the amount of reflected/absorbed power by a Silicon, Boron doped, polished target was dependent upon the angle of the target with the incident laser beam.

D. PULSE SYSTEM LASER DESIGN

The design of a system that will enable the pulsing and the increase in output power of the NPS HF/DF laser is of concern for the measurement of laser target interaction and the comparison of those measurements with previously reported measurements of a Neodymium glass laser by Chenoweth and Johnson in reference 12. By obtaining a high power, short duration pulse, laser target interaction measurements can be taken.

The basic idea of the design is founded upon the fact that not all the SF_6 in the discharge flow is being dissociated by the applied input voltage. By dropping a high voltage of short duration across the anodes of the laser while there is flow across those anodes it is hoped that more SF_6 can be dissociated so that there will be more free fluorine radicals available for reaction with the H_2 injected into the laser cavity. Further discussion of this design will be given in chapter 4.

Figure 3.9 shows the design recommended for wiring and testing to pulse the NPS HF/DF laser. From the figure it can be seen that three high voltage vacuum switches will be needed as well as a 15 kΩ resistor rated at 225 Watts. A variable resistance is also shown and will be discussed in chapter 4. A connection from the high voltage tank for the #1 HV (high voltage) vacuum switch in series with the 15 kΩ resistor to the capacitor bank must be accomplished. There must also be a connection on the same output line from the high voltage (HV) tank for the #3 HV vacuum switch to the

Once the pulsing has been accomplished for the laser, target interaction and damage measurements can be obtained for Boron doped Silicon targets. These measurements can be compared and contrasted to the measurements given for the Nd laser by Chenoweth and Johnson in reference 12.

Another important feature is that the discharge flow of the gases is exhausted to atmosphere without being totally utilized in the gain zone of the laser. A design for a system that would recirculate the gases back into the cavity and through the gain zone would be beneficial in extracting more of the free fluorine radicals and unused H_2 for increasing the amount of excited HF^*. This would require chemical separation of all the reactants. Some O_2, H_2, and all the He should be recoverable and need not be separated. The fraction of SF_6 to be recovered should be determined.

Lastly, the further experimental observations of the operating characteristics of the HF/DF laser should be investigated utilizing the new power supply. In particular, an 85 percent reflectance mirror should be obtained and measurements taken for power output as a function of flow rate. Funk and Sontheimer found that by using the 85 percent reflectance mirror their power output increased from 1.6 Watts to 6 Watts. Based upon this data a predicted power output with the new power supply would be approximately 9 Watts.

angle of the beam to the target increased the power reflected increased and the power absorbed decreased. The angle at which there was found to be maximum reflection was 60 degrees. The data for the target angle of 65 degrees is in error and does not follow the trend of increased reflectivity with target angle. This error is most probably due to a misalignment of the detector measuring the reflected power from the target. We would expect that the power reflected would increase with target angle and when a grazing is approached the maximum power reflected would occur. We would also expect to find that the maximum power absorbed would occur when the target is normal to the beam. The data taken is in agreement with these expected results.

C. PULSE SYSTEM DESIGN

The design of the system to pulse the HF/DF laser is described in chapter 3. It will pulse the laser dependent on the variable resistance that should be experimentally determined. The variable resistance can be tested at several different settings to obtain an optimum time of discharge for the capacitor bank. Power measurements with different resistor settings should be taken in order to find the optimum resistor setting for the maximum amount of power output per pulse. This is only a conceptual design for pulsing the HF/DF laser and should only be used as a basis for upgrading the present laser system.

D. RECOMMENDATIONS FOR FURTHER STUDY

The first and primary recommendation for further study is to rewire the power supply to a capacitor bank via vacuum high voltage switches in order to obtain a pulse system configuration of the HF/DF laser. The design is discussed in chapter 3.

IV. CONCLUSIONS

A. LASER OPERATING CHARACTERISTICS

The final results of the operating characteristic measurements of the HF/DF laser at NPS were in general agreement with the previously reported data by Spencer, Beggs, and Mirels [Ref. 3] as well as with Funk and Sontheimer [Ref. 9]. The major accomplishment of performing these measurements was found to be that the replacement of the previous power supply with the Hipotronics power supply increased the power output of the laser. This was accomplished by the ability to raise the discharge voltage from 15.7 kV to 19.0 kV. This increase in voltage caused a higher amount of SF_6 to be dissociated thus allowing for a greater power output.

The optimum flow rates of the various gases were found to change with the change in optimum input voltage. These new flow rates were found to be:

1. SF_6 = .7167 grams/second
2. H_2 = .0220 grams/second
3. O_2 = .2200 grams/second
4. He = .0500 grams/second

These flow rates as well as the 19 kV input voltage yielded an output power fluctuating between 2.00 and 2.46 Watts with a maximum output power of 2.60 Watts reported. This power increase is approximately 60 percent better than the previously reported data of Funk and Sontheimer.

B. POWER VARIATION WITH TARGET ANGLE

The effect of target angle upon the amount of power reflected/absorbed by the target was substantial. As the

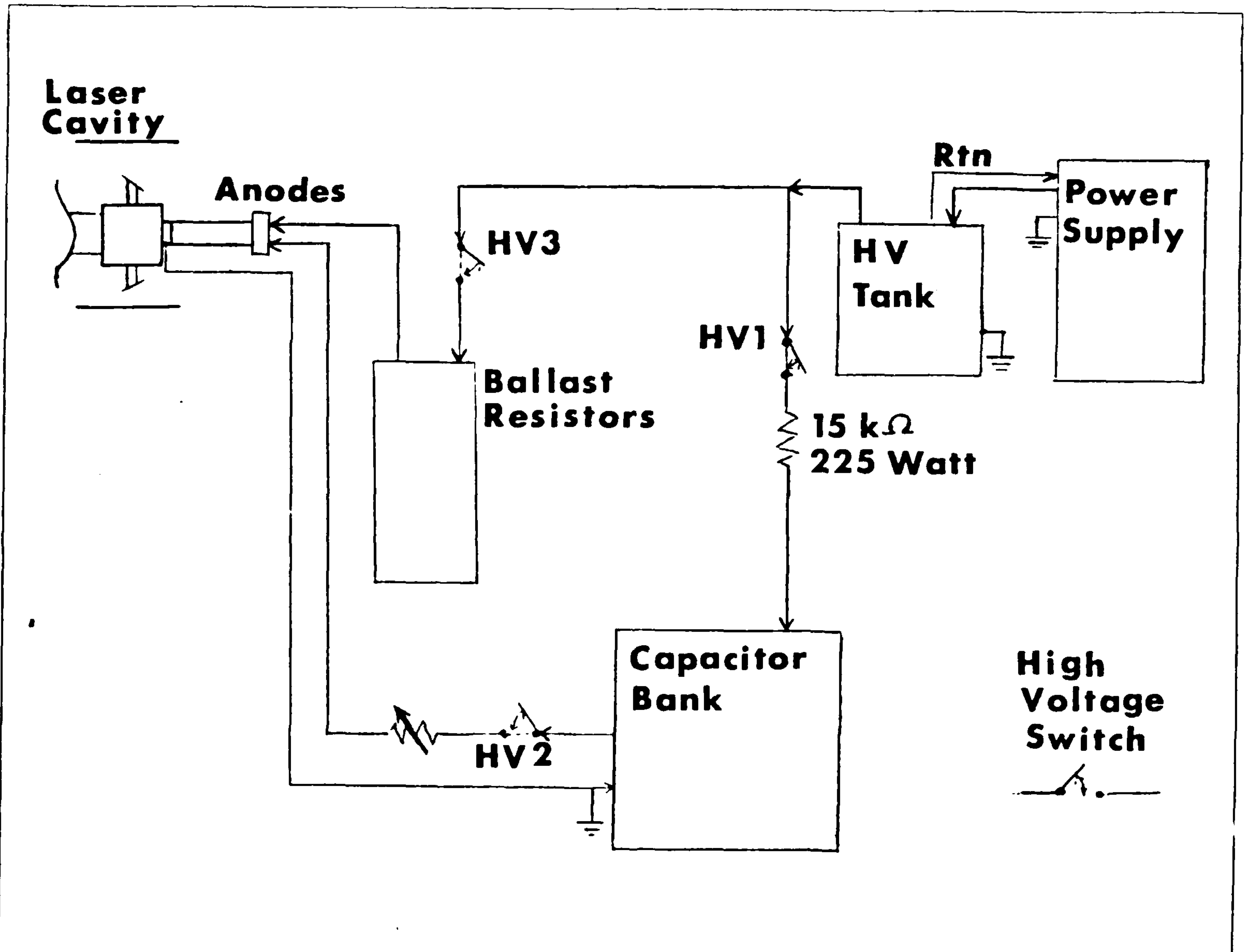

Figure 3.9 HF/DF Pulse Laser System Design

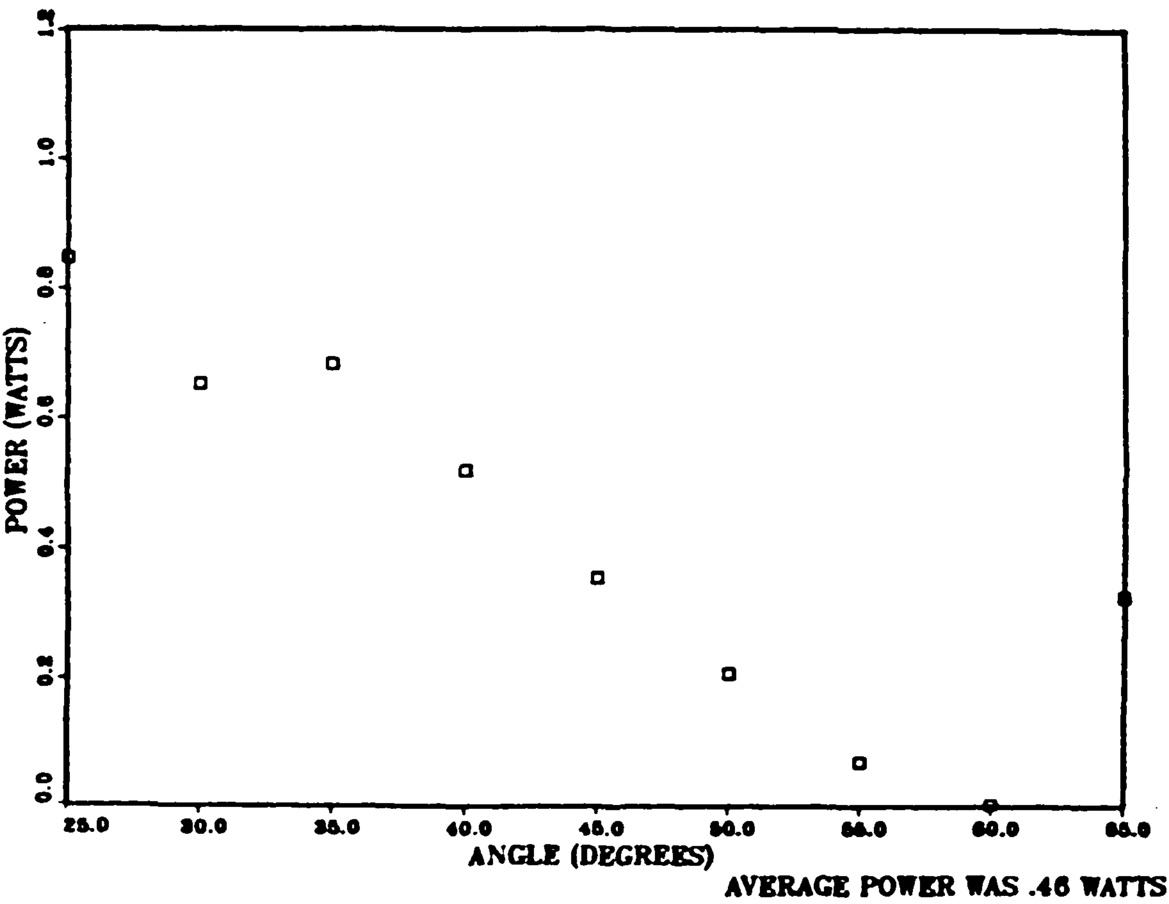

Figure 3.8 Power Absorbed vs Target Angle

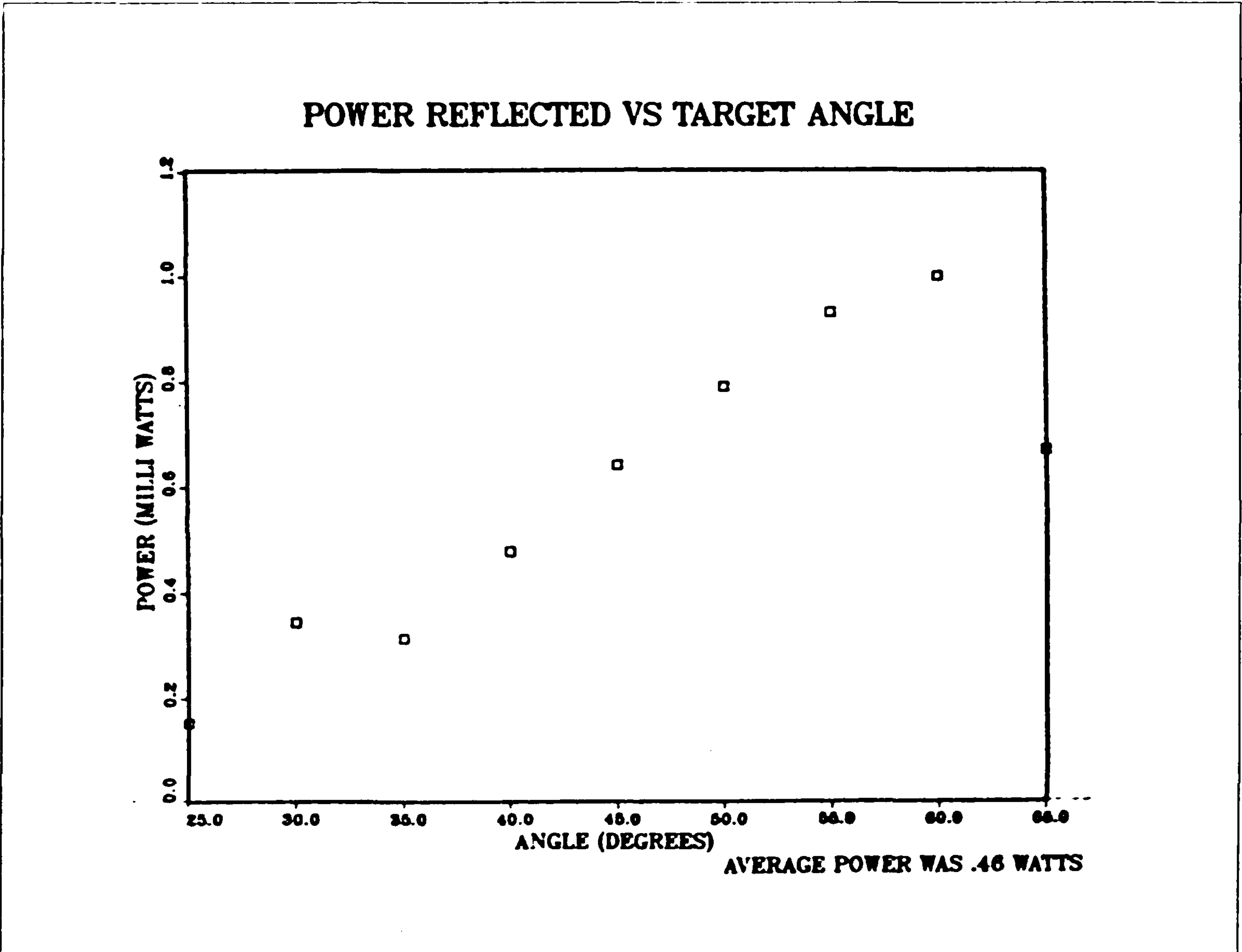

Figure 3.7 Power Reflected vs Target Angle

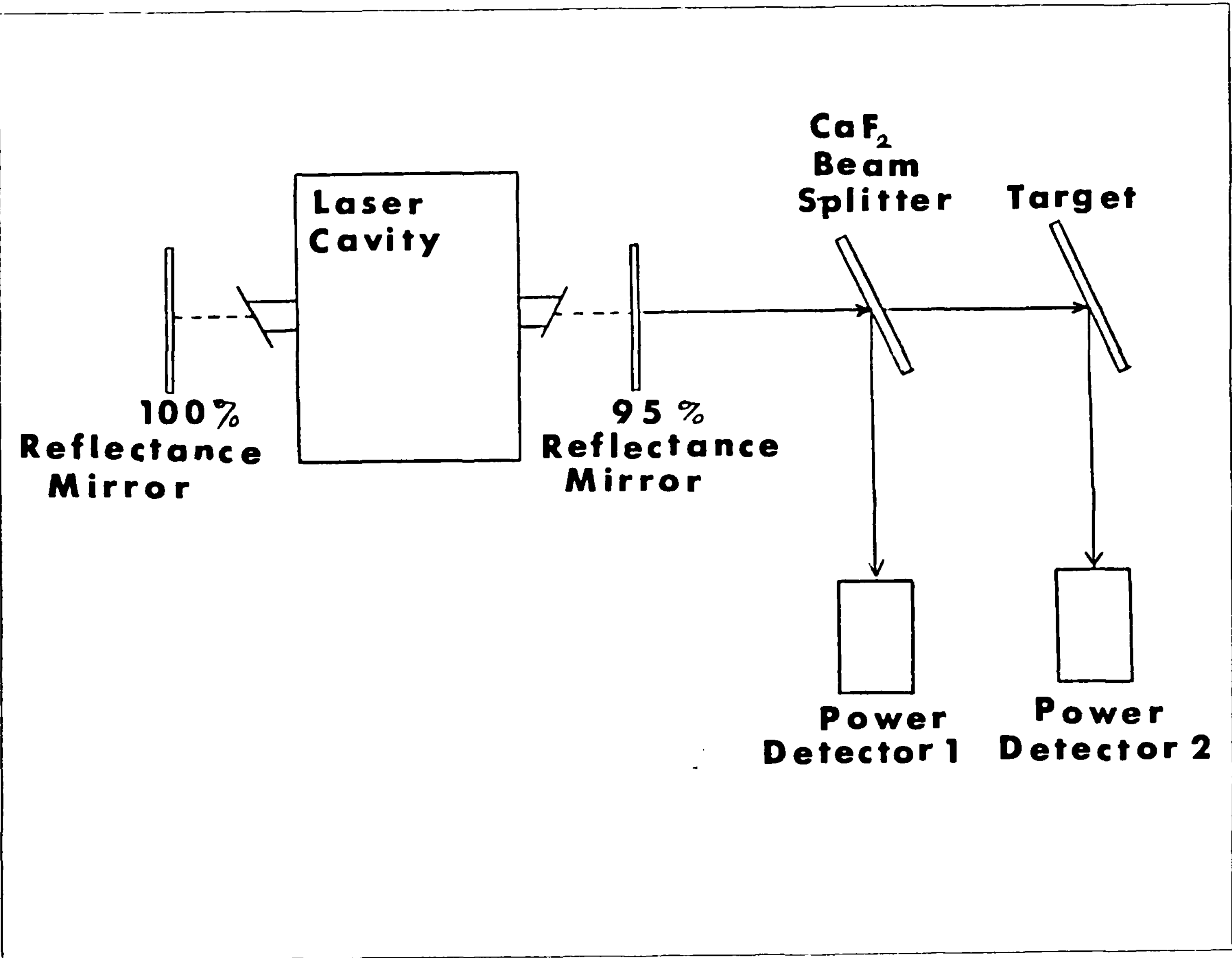

Figure 3.6 Laser/Target Interaction Diagram

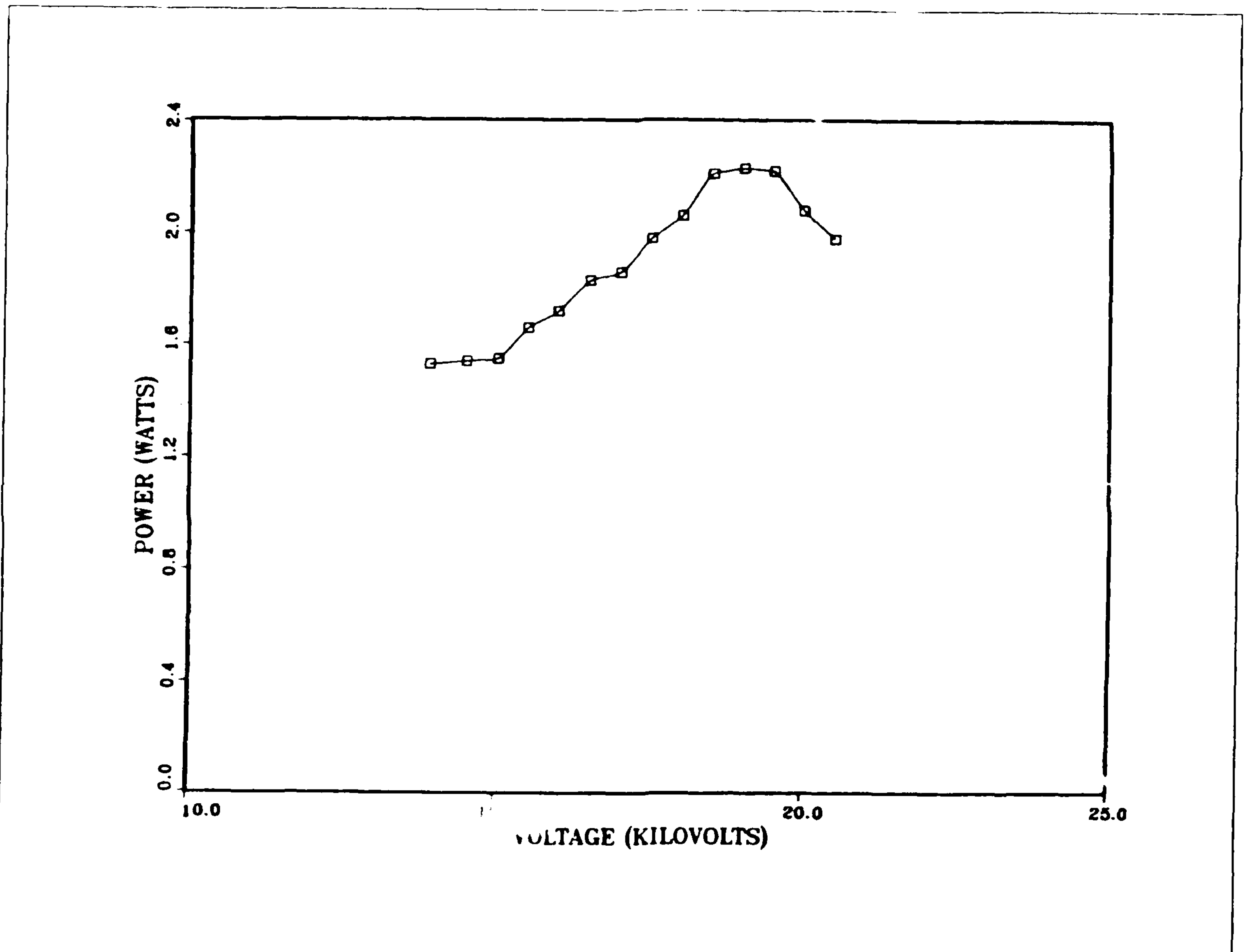

Figure 3.5 Power Variation with Input Voltage

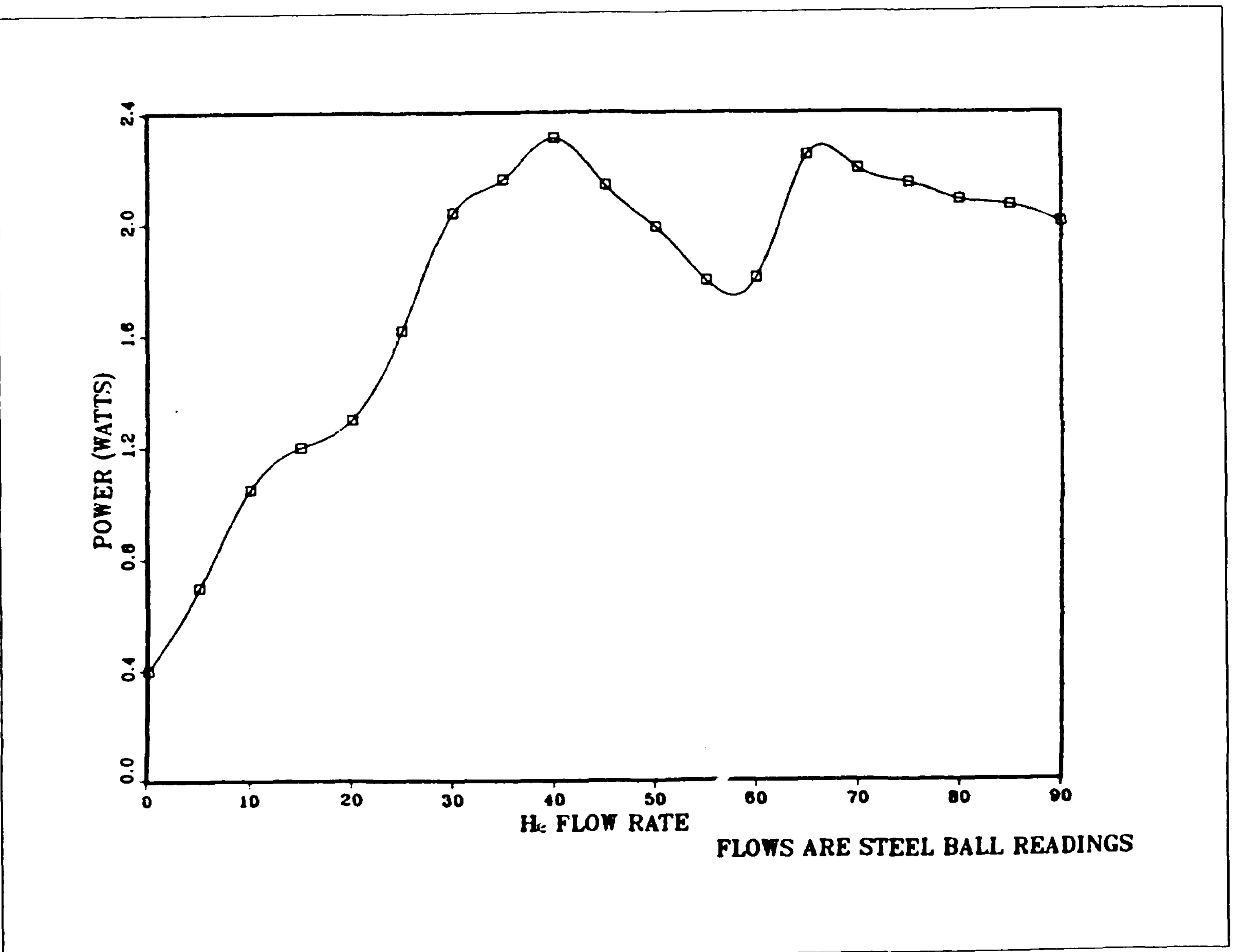

Figure 3.4 Power Variation with He Flow

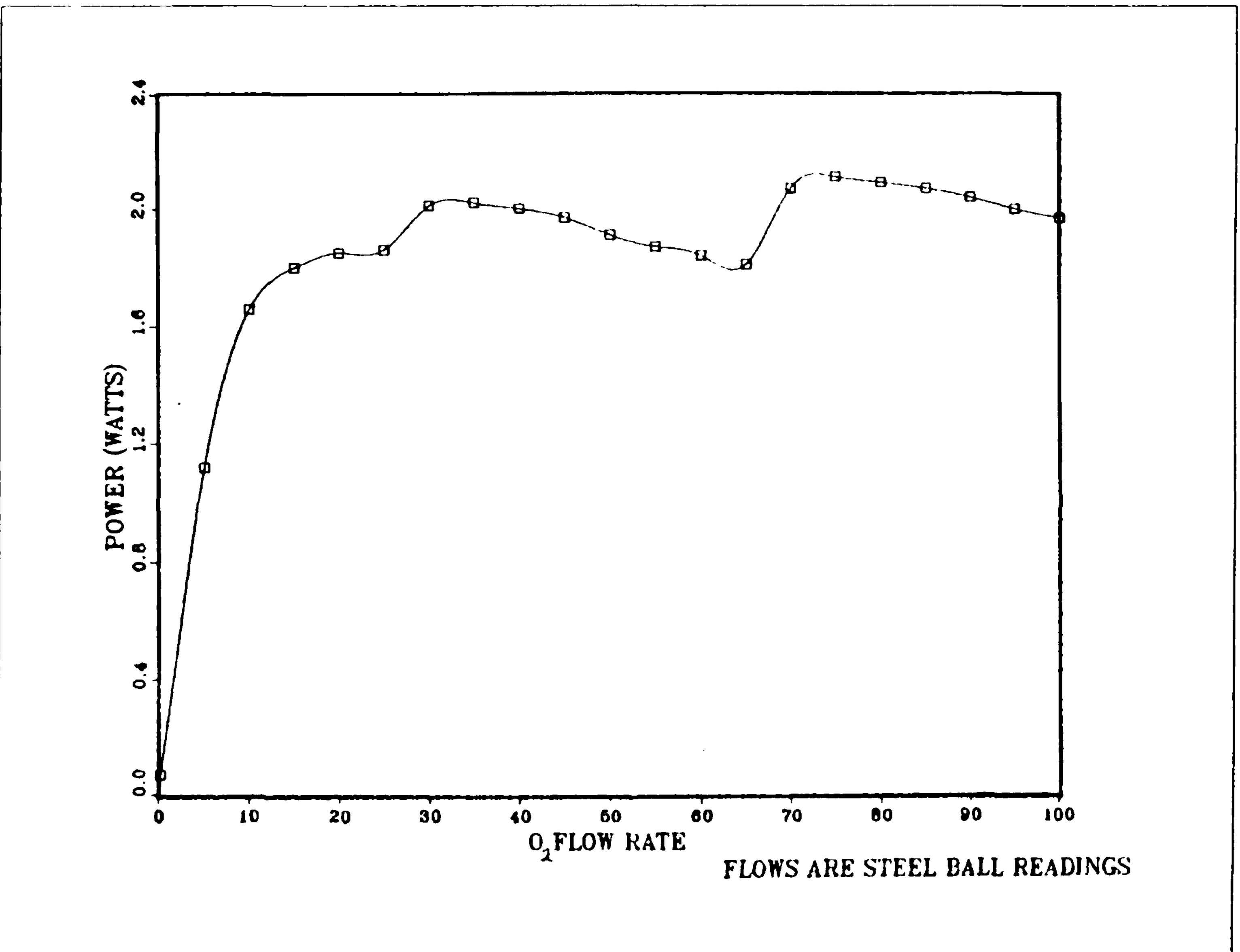

Figure 3.3 Power Variation with O_2 Flow

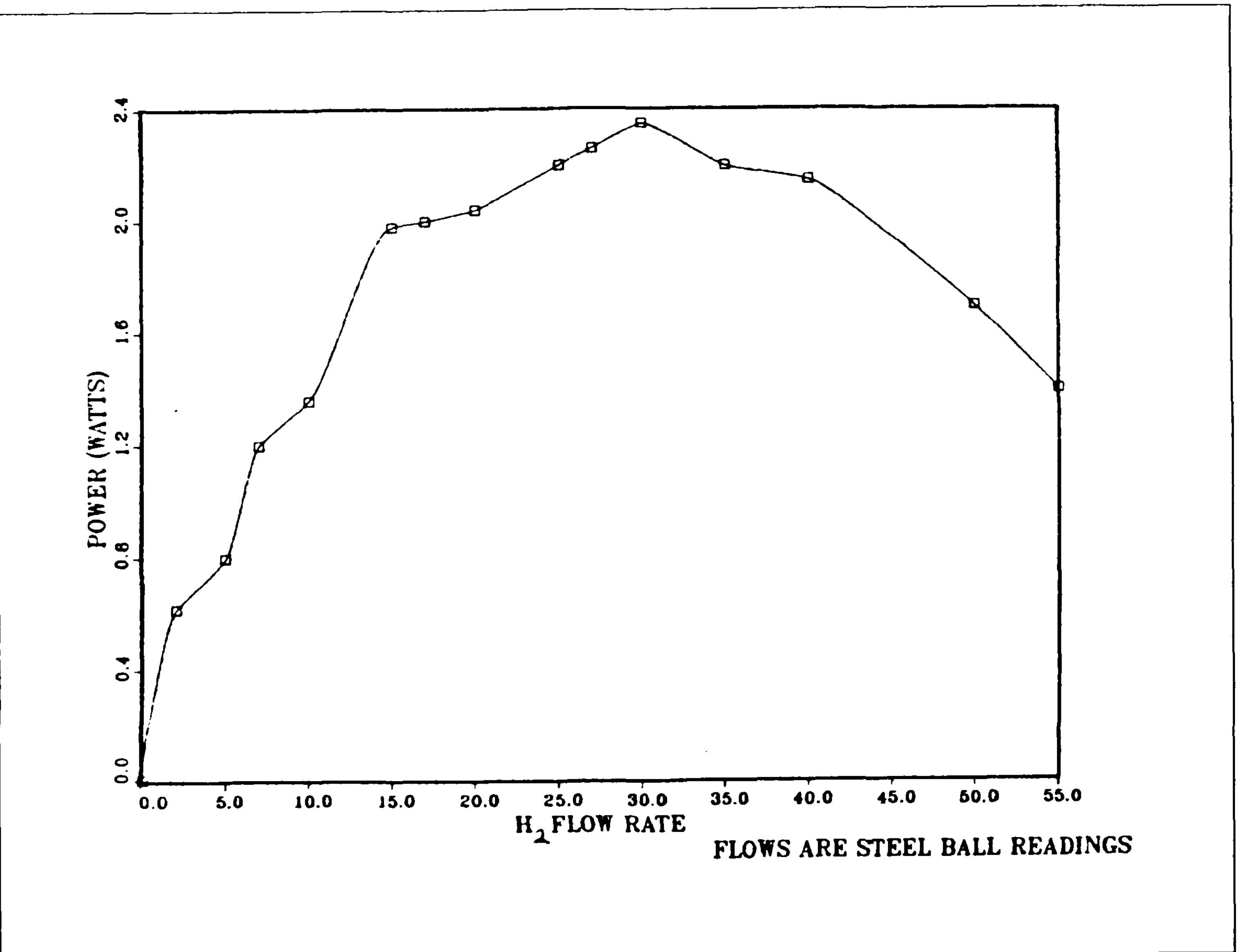

Figure 3.2 Power Variation with H_2 Flow

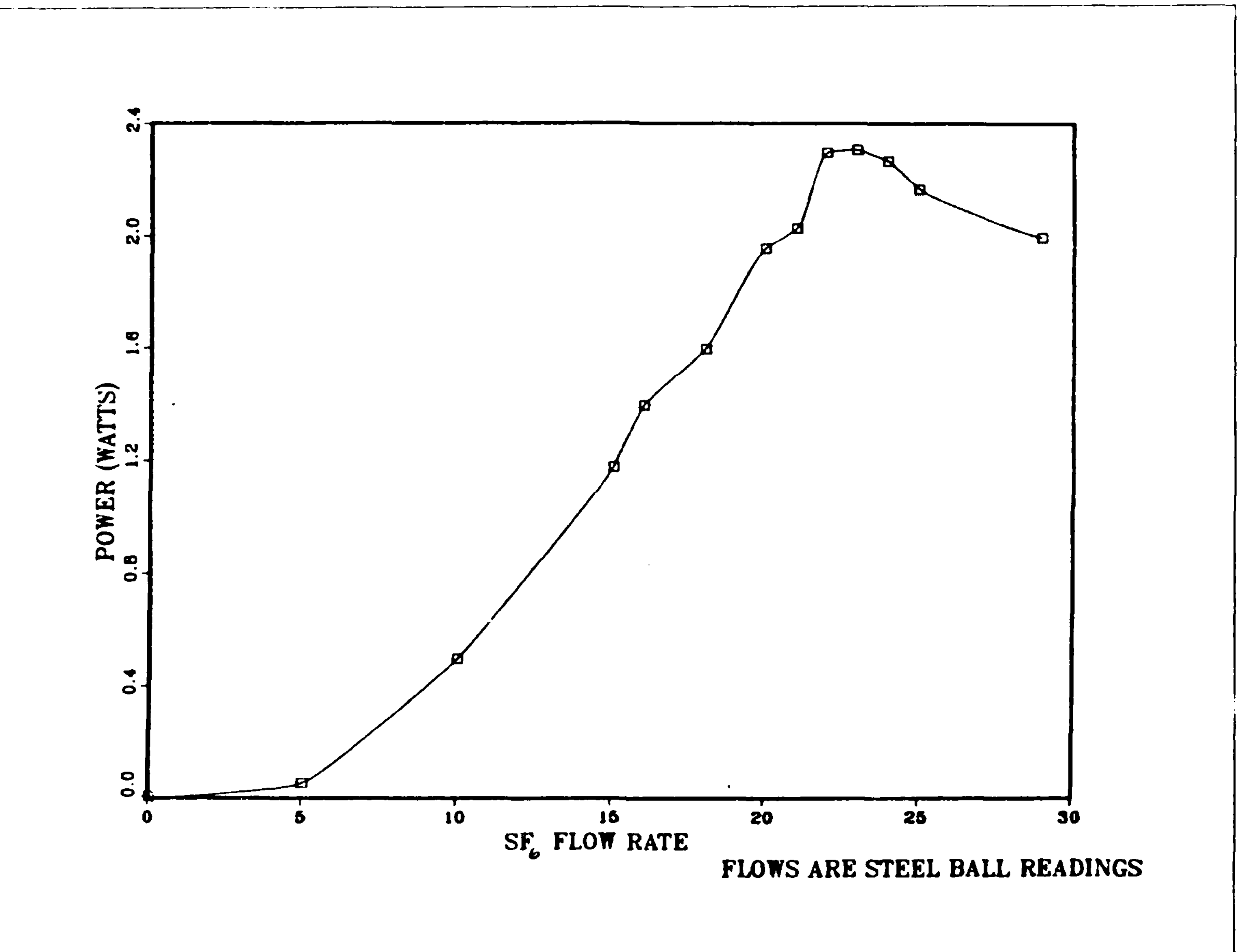

Figure 3.1 Power Variation with SF_6 Flow

TABLE IV

Approximate Flow Rates for Steel Ball Readings

STEEL BALL READING	He (g/s)	O_2 (g/s)	H_2 (g/s)	SF_6 (g/s)
0	0	0	0	0
2	.0017	.0067	.0010	.0100
4	.0033	.0133	.0025	.0900
5	.0050	.0200	.0033	.1000
6	.0067	.0267	.0040	.1617
8	.0083	.0333	.0055	.2233
10	.0100	.0400	.0070	.2850
12	.0132	.0440	.0085	.3590
15	.0163	.0500	.0108	.4700
18	.0194	.0590	.0130	.5933
20	.0225	.0650	.0145	.6550
21	.0229	.0700	.0158	.7167
23	.0234	.0750	.0170	.7783
25	.0238	.0800	.0183	.8400
30	.0250	.0950	.0220	1.0250
35	.0300	.1000	.0258	1.2100
40	.0350	.1150	.0295	1.3950
45	.0380	.1300	.0333	1.5800
50	.0400	.1450	.0370	1.7650
55	.0425	.1600	.0408	
60	.0450	.1750	.0445	
65	.0500	.1900	.0483	
70	.0538	.2050	.0520	
75	.0575	.2200	.0558	
80	.0600	.2350		
85	.0625	.2500		
90	.0650	.2650		
95	.0675	.2800		
100	.0700	.2950		

ballast resistors. An additional line must be connected via the #2 HV vacuum switch and a variable resistance, to be determined, to the eight anode connections of the discharge tube.

The operation of the design would be simple. First the flow rates of the gases could be set by closing HV # 1 and opening HV # 2 and #3. This allows for application of high voltage to the discharge tube for setting of the flow rates for an optimum lasing condition. Next the high voltage would be secured and HV # 3 would be opened and HV # 1 would be closed. HV #2 would remain closed while the charging of the capacitor bank was being accomplished. Application of the high voltage would then charge the capacitor bank with the 15 kΩ resistor ensuring that it would be done slowly. Once the capacitor bank is charged HV # 1 would be opened and then HV # 2 would be closed. The closure of HV #2 would discharge the voltage stored in the capacitor bank across the eight anodes in the discharge tube. The variable resistance could be utilized to control the time it takes for the capacitor bank to discharge. This design should allow the use of the HF/DF laser as a pulse laser.

APPENDIX A

START UP PROCEDURES

1. Turn vacuum pump coolant water on.
2. Insert key into security lock and energize.
3. Energize vacuum pump.
4. Open scrubber vacuum roughing valve slowly.
5. Open all gas cylinder valves at the regulators.
6. Energize ballast resistor cooling fans and cavity cooling pump.
7. Energize high voltage power supply.
8. Apply high voltage to discharge tube.
9. Turn on He to desired flow rate.
10. Turn on SF_6 to desired flow rate slowly.
11. Turn on O_2 to desired flow rate.
12. Turn on H_2/D_2 to desired flow rate.
13. Vary the cavity vacuum roughing valve to the desired pressure.

APPENDIX B

SHUT DOWN PROCEDURES

1. Secure high voltage.
2. Close H_2,O_2, and SF_6 gas cylinder regulator valves.
3. Close He flow valve on gas control panel.
4. Pump down H_2,O_2, and SF_6 to clear lines.
5. When lines have cleared secure scrubber vacuum roughing valve.
6. Open He flow valve to fill cavity up to one atmosphere He. (Relief valve on vacuum gauge opens at 15 psi).
7. Secure He gas cylinder regulator valve.
8. Allow about five minutes to cool down ballast resistors and cavity cooling water.
9. Secure ballast resistor cooling fans and cavity cooling pump.
10. Secure vacuum pump power.
11. Turn off vacuum pump cooling water.
12. Turn security lock to off position and remove key.

APPENDIX C
LASER CAVITY ALIGNMENT

1. Take out the output coupling mirror (M_2) and cover the 100 percent reflectance mirror (M_1).

2. Energize the laser with all the gas flows and the discharge voltage set at the optimum conditions.

3. Observe the location of the hydrogen-fluorine flame, about 1.5 mm downstream of the hydrogen injection ports.

4. Secure the laser, replace M_2, and uncover M_1.

5. Set up a He-Ne (28 Å) alignment laser and a beam-splitter (microscope glass slide) as shown in reference 6.

6. Place a piece of white paper in front of M_2 and position the He-Ne laser beam through the cavity, unobstructed, at the point determined in step 3 above.

7. Adjust M_2 to reflect the beam back through the cavity at the flame location.

8. Place a piece of white paper in front of M_1 and optimize the beam on M_1.

9. Remove the paper from M_1 and reflect the beam back through the cavity and strike M_2 in the same position that the original beam was incident upon M_2.

10. Step 9 is critical and must be within 0.8 mm for lasing to occur, therefore, place an index card with a 1 mm hole in it in front of M_2 with the original beam going through the hole.

11. Adjust M_1 until the reflected beam is incident upon the hole.

12. Energize the laser with all the gas flows and the discharge voltage set at the optimum conditions.

13. Observe the power meter for indication of lasing.

14. Repeat steps 4 through 14 until the presence of lasing is observed.

15. Once lasing has been established obtain required measurements.

LIST OF REFERENCES

1. Wilson, L.E., "Deuterium Fluoride CW Chemical Lasers", Proceedings of the Society of Photo-optical instrumentation Engineers, v. 76, p. 51-57, March, 1976

2. Gross, R.W.F. and Spencer, D.J., Continuous Wave Hydrogen Halide Lasers, unpublished paper, Aerospace Corporation, El Segundo, Ca., 1974

3. Spencer, D.J., Beggs, J.A. and Mirels, H., "Small-scale CW HFDF chemical laser", Journal of Applied Physics, v. 48, no. 3, p. 1206-1211, March, 1977

4. Cool, T.A., Stephens, R.R. and Shirley, J.A., "Power and Gain Characteristics of High Speed Flow Lasers", Journal of Applied Physics, v. 41, p. 4038, 1970

5. Hinchen, J.J., "CW HF Electric-Discharge Mixing Laser", Journal of Applied Physics, v. 45, p. 1818, 1974

6. Funk, W.T. and Sontheimer, R.F., A Hydrogen Fluoride/Deuterium Fluoride Laser at the Naval Postgraduate School, M.S. Thesis, Naval Postgraduate School, Monterey, Ca., June, 1977

7. Cooper, A.W. and Crittenden, E.C. Jr., High Power Lasers and Effects, unpublished notes (chapter II), Naval Postgraduate School, Monterey, Ca., 1977

8. Avizonis, Petras, "Carbon Dioxide Electrical and Gas Dynamic, HF Chemical Gas Lasers", High Energy Lasers and their Applications, v. 1, p. 272-290, 1974

9. Emmanuel, G. and Whittier, J.S., Closed Form Solution to Rate Equations for an F + H Laser Oscillator, Aerospace Corporation Report on Contract F04701-71-C-0172, 1972

10. Fuhs, A.E., High Energy Laser System Design, Department of Aeronautics, Naval Postgraduate School, Monterey, Ca., forthcoming

11. Mirels, H. and Spencer, D.J., "Power and Efficiency of a Continuous HF Chemical Laser", IEEE Journal of Quantum Electronics, v. QE-7, no. 11, November, 1971

12. Chenoweth, E. L. and Johnson, G. D., Time-Resolved Reflectivity Measurement of Extrinsic Silicon during Pulsed Laser Irradiation, M.S. Thesis, Naval Postgraduate School, Monterey, Ca., June 1984.

INITIAL DISTRIBUTION LIST

		No. Copies
1.	Chairman, Dept. of Physics Code 61 Naval Postgraduate School Monterey, California 93943	2
2.	Library Code 0142 Naval Postgraduate School Monterey, California 93943	2
3.	Dr. A. W. Cooper Code 61Cr Naval Postgraduate School Monterey, California 93943	2
4.	Dr. E. A. Milne Code 61Mn Naval Postgraduate School Monterey, California 93943	2
5.	Lt. Edward Lee Garcia, USN SSPO Lockheed Aerospace Corporation Sunnyvale, California 94089	1
6.	Bob Sanders Code 61Rs Naval Postgraduate School Monterey, California 93943	1
7.	Defense Technical Information Center Cameron Station Alexandria, Virginia 22314	2

END

FILMED

5-85

DTIC